The Glaciofluvial Environment of Linnébreen, Spitsbergen, Svalbard

Senior Thesis

presented by

Simon L. Pendleton

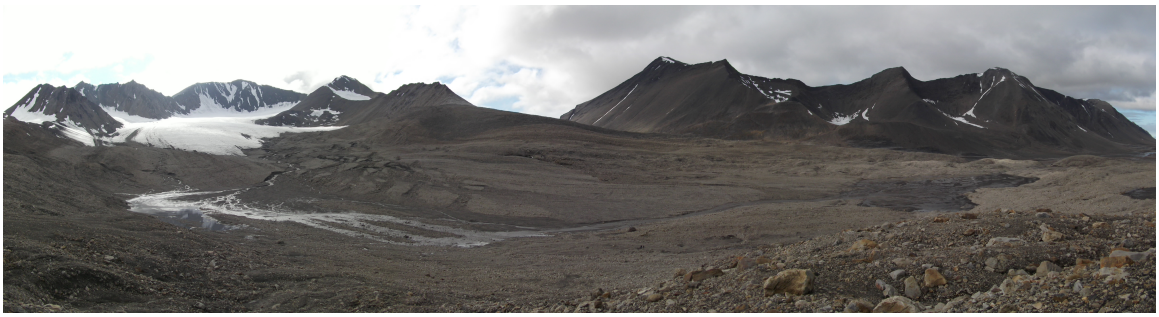

Department of Geology, Environmental Studies Program
Whitman College

May 2011

Certificate of Approval

This is to certify that the accompanying thesis by Simon L. Pendleton has been accepted in partial fulfillment of the requirements for graduation with Honors in Geology / Environmental Studies

_____

Dr. Robert J. Carson

Whitman College
May 8, 2011

Table of Contents

List of Figures

Abstract

Suspended sediment concentrations (SSC), meltwater discharge and local climatic conditions of the Linné glaciofluvial system were monitored from July 21 to August 9, 2010 in order to determine the temporal relationships between local climate, glacier melting and sediment production. ISCO water samplers were installed along the main meltwater channel to record SSC. SSC was directly related to discharge of the glaciofluvial system, which was in turn dependent on melt of the Linné glacier. The relationship between SSC and climatic conditions can be linked to the rate of glacier melt, which is in turn controlled by local climatic conditions. Of all the observed weather conditions, precipitation had the highest impact on glacier melt and discharge and therefore had the highest correlation to SSC. During periods without precipitation, solar radiation was the greatest influence on glacier melt and SSC. Measured SSC and calculated sediment load for the season from the Lower (distal) site was substantially less than the measured SSC and calculated sediment load at the Upper (proximal) site. The differences between the two sampling sites indicate that the glaciofluvial system immediately downvalley of the glacier is acting as a sediment sink. This study has established that increased SSC is largely due to increased precipitation. The presence of a pro-glacial sediment sink interrupts the sediment signal produced by the glacier and complicates the sediment record downvalley in Lake Linné.

1. Introduction

Global climate change is especially pronounced in the high Arctic. Small variations in global weather patterns have a disproportionately large effect on both the local and regional climate, likely due to a number of positive feedback effects including cloud dynamics and decreasing surface albedo from melting ice and snow (Overpeck et al. 1997). It is this climatic sensitivity that makes the Arctic an excellent indicator of local, and indirectly, of global climate trends. In an age when anthropogenic climate change concerns are becoming paramount, the Arctic presents a unique natural laboratory to study past and present climate conditions to better understand what the future will bring.

Due to this climate sensitivity, and how changes in climate affect sediment production in glacial systems, high Arctic lakes are capable of producing high-resolution paleoclimate records (Snyder et al. 1999; Braun et al. 2000). The glaciolacustrine system of Lake Linné, located on the west coast of Spitsbergen, Norway contains one such record. Though reading these lake sediments as a record of past climate is the long-term goal of the Svalbard Research Experience for Undergraduates (REU) project, in order to understand the cored sediment layers, the source and transport mechanisms of that sediment must also be understood. The goal of this project is to characterize the glaciofluvial environment and measure the sediment flux emanating from the Linné glacier. By understanding how the Linné glacier, the major sediment source of Lake Linné, responds to variations in climate, we hope to better understand the correlation between the sediment record and paleoclimate.

1.1. Svalbard REU Program

The long-term goal of the Svalbard REU program is to interpret the sedimentation record of Lake Linné as a high-resolution paleo-climate record. The lake sediments consist of rhymites of dark, fine-grained, and light, coarser-grained layers, with each pair interpreted as one year's sediment accumulation. Since the summer of 2004, the undergraduate researchers and program advisors from the Svalbard REU have been working in the Linné valley, characterizing the climatic, glacial, and fluvial processes affecting sedimentation in Lake Linné. Ultimately, the program hopes to use the combined research of the students and advisors to provide substantive correlation between meteorological conditions and subsequent sedimentation in Lake Linné, which will allow us to read the lake sediments as a record of past climate with a higher degree of certainty. Through understanding the relationship between climate and the representative sediments, this study can hopefully act as a basis for deconstructing paleoclimate in other areas; both in the high Arctic and elsewhere.

1.2. The Climate-Glacier-Sediment System

In linking climate to sediment deposition in Lake Linné, three key elements must be understood: climate effects on the sediment source (the glacier) and how those changes affect sediment production, how the fluvial system affects the sediment, and deposition of sediment in the lake (Figure 1). Previous work by Hodson (1994) on similar glaciofluvial systems in Svalbard has shown that the glacier is the main sediment input for the fluvial and lacustrine system, and that the smaller tributaries have a neglible influence on the lacustrine sediment record.

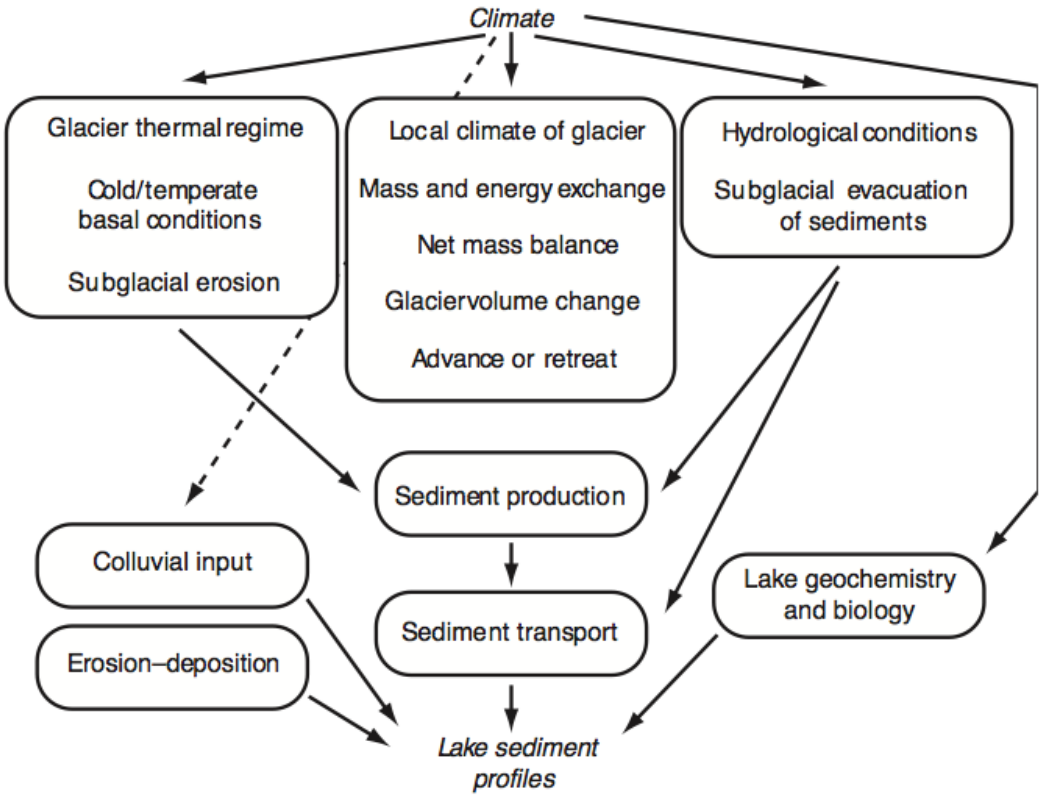

Figure 1: Flowchart depicting the relationship between climate, glacier, sediment production, transport and deposition in a galciolacustrine system (Jansson et al. 2005) .

Previous work by Mattel (2006) showed that the river connecting the source (the Linné glacier) and the ultimate depositional environment (Lake Linné) was a sediment sink. Mattel also concluded that suspended sediment concentration (SSC) was transport-limited, not supply–limited: the limiting factor in sediment yield was discharge, not amount of sediment available. Mattel work showed that while the proglacial area was responsible for a majority of the sediment produced in the Linné valley, the Linné river with its broad braid plains (Figure 4a) acted as a sediment sink and therefore masked any short-term sediment signal given off by the glacier. Long-term climate variations, and thus changes in sediment production from the Linné glacier, are recorded in Lake Linné, but the short-term signal is dominated by sediment influxes from the Linné river caused by precipitation driven, high discharge events (Matell 2006).

Hodgkins and others (2003) who performed extensive SSC monitoring of Finsterwalderbreen, a similar galciofluvial system in Svalbard, also found that the majority of sediment yield was produced during discrete high discharge events. They also concluded that net sediment production from a glaciofluvial system occurred during years of sustained transport, higher discharge, and therefore higher precipitation.

1.3. Individual Research

Matell (2006) worked to characterize the parameters of Linnéelva, the system responsible for transport of sediment from its source to its eventual deposition, (Figure 1). In 2010, other members of the REU investigated cores taken from Lake Linné. However, the mechanisms of the major source of sediment for Lake Linné, Linné glacier, are yet to be fully understood. The purpose of this study is to

characterize the fluxes in sediment output from Linné glacier and its proglacial environment. By monitoring SSC and local climate conditions simultaneously, it is possible to correlate weather events and changes in sediment output. SSC is one of the most sensitive proxies of environmental change in glaciated catchments because it is directly linked to transport mechanisms, which are controlled by glacier melt and thus local climatic conditions (Hodgkins et al. 2003). Through categorizing the temporal patterns of sediment production and storage in the proglacial environment, a better understanding of sediment production from Linné glacier as well as deposition in Lake Linné, and how these sediment patterns record climate data, can be established.

1.4. Setting

Svalbard is an archipelago between 74° and 81° north latitude and 10° and 35° east longitude (Figure 2). The study site, the Linné valley, is located on the west coast of Spitsbergen, the largest island of the archipelago (Figure 2). Spitsbergen is characterized by glacially eroded valley and fjord systems divided by steep mountains. Roughly 60% of Svalbard is glaciated, consisting mostly of small valley glaciers, though large ice caps are present on the eastern islands of Edgeøya, Barentsøya, and Nordaustlandet (Figure 2). The cooler, drier climate of interior Spitsbergen produces relatively small cold-based valley glaciers that move only 1-2 m per year, while the more humid areas along the coast (like the Linné valley) produce polythermal glaciers, which move between 10-30 m a year (Ingólfsson 2004).

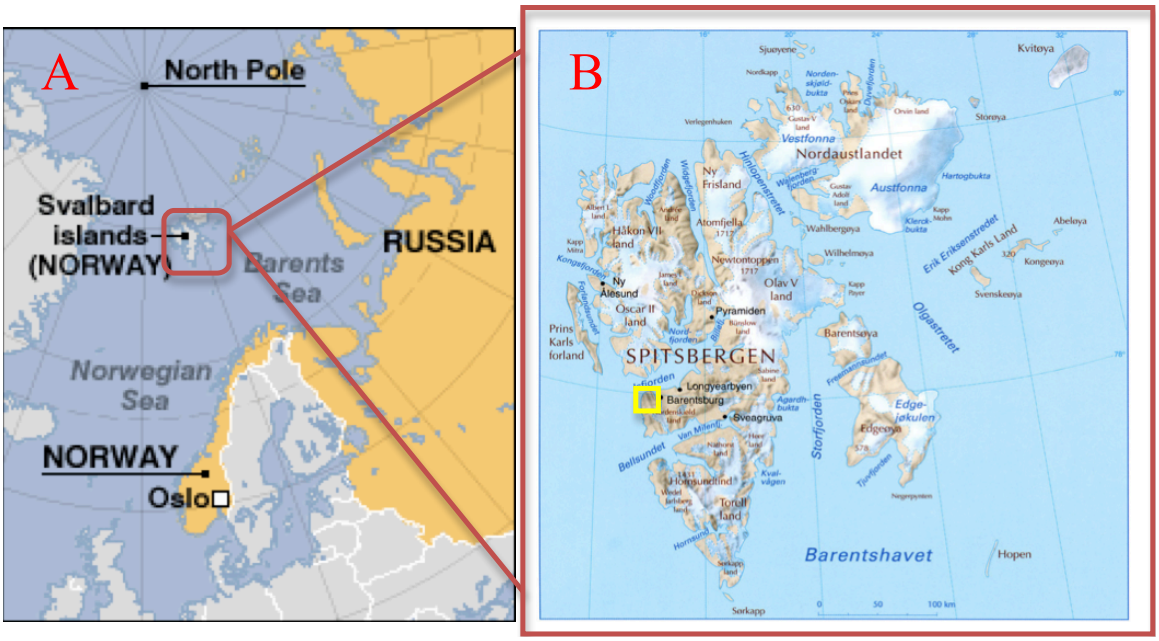

Figure 2: a) Location of Svalbard archipelago (2010) b) Svalbard with study site outlined in yellow (Thasler 2010).

Located well north of the Arctic Circle, the modern climate of Svalbard is maritime polar. Mean annual air temperatures hover around -6°C at sea level and can dip as low as -15°C in the high mountains of central Spitsbergen. Weather records from Longyearbyen show February to be the coldest month on average at -15.2°C, while July is the warmest with a temperature of 6.2°C (Ingólfsson 2004). The dominant type of precipitation is snow; the dryer interior receives roughly 200 mm per year, while the humid coasts receives 400-600 mm per year. The border between the cold arctic air of the Polar Basin to the north and the mild oceanic air from the Barents Sea runs through Svalbard, causing high winds and precipitation along the coasts (Ingólfsson 2004).

The modern arctic climate of Svalbard allows for a permanent periglacial environment with continuous permafrost extending over almost the entire area of Svalbard. Near the coast, where the ocean moderates the milder climate, permafrost

is 10-40 m thick, but in the colder interior and highlands, permafrost is up to 450 m thick. Periglacial geomorphic processes and features are more prevalent in western regions where solifluction lobes, and patterned ground such as sorted stone circles and stripes are pervasive and well developed (Figure 3) (Ingólfsson 2004).

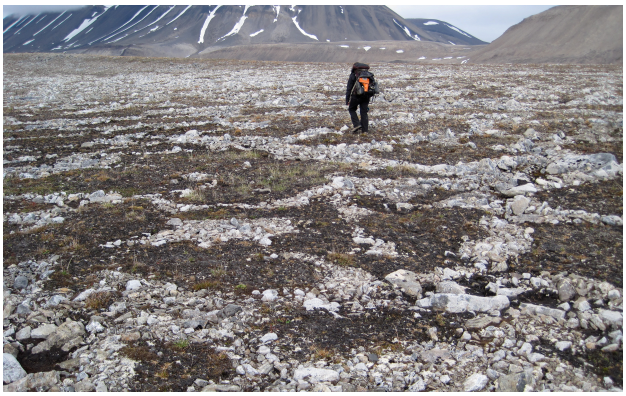

Figure 3: Stone circles in the Linné valley.

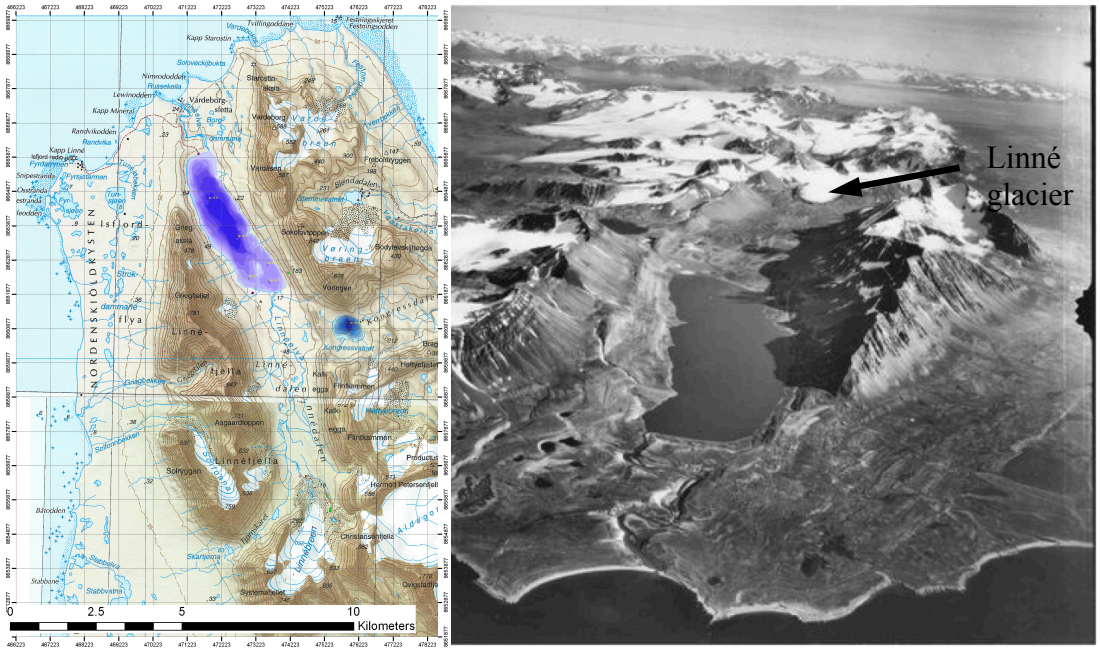

Figure 4: a) Topographic map of Kapp Linné and the Linné valley; b) Oblique aerial photo looking south up the Linné valley with Lake Linné visible in foreground and the Linné glacier at head of valley. Images courtesy of Norsk Polarinstitutt.

1.4.1. Linné valley

The Linné valley, located at 78˚03’ north and 13˚50’ east on the west coast of Spitsbergen (Figure 2, Figure 4), is a glacially eroded former fjord that was deglaciated sometime just prior to 12,300 BP before being inundated by rising sea level (Mangerud et al. 1990; Snyder et al. 1999). Radiocarbon dates of Lake Linné sediments show a change in depositional environment from marine to lacustrine dating to approximately 9,500 BP, representing a falling sea level and isolation of the fjord (Mangerud et al. 1990; Snyder et al. 1999). Lake Linné formed from glacial overdeepening of Linné valley during Late Weichselian glaciation (Snyder et al. 1999). Lake Linné is 4.6 km^2 in area, with a maximum depth of 37 m, and drains a 27 km^2 catchment.

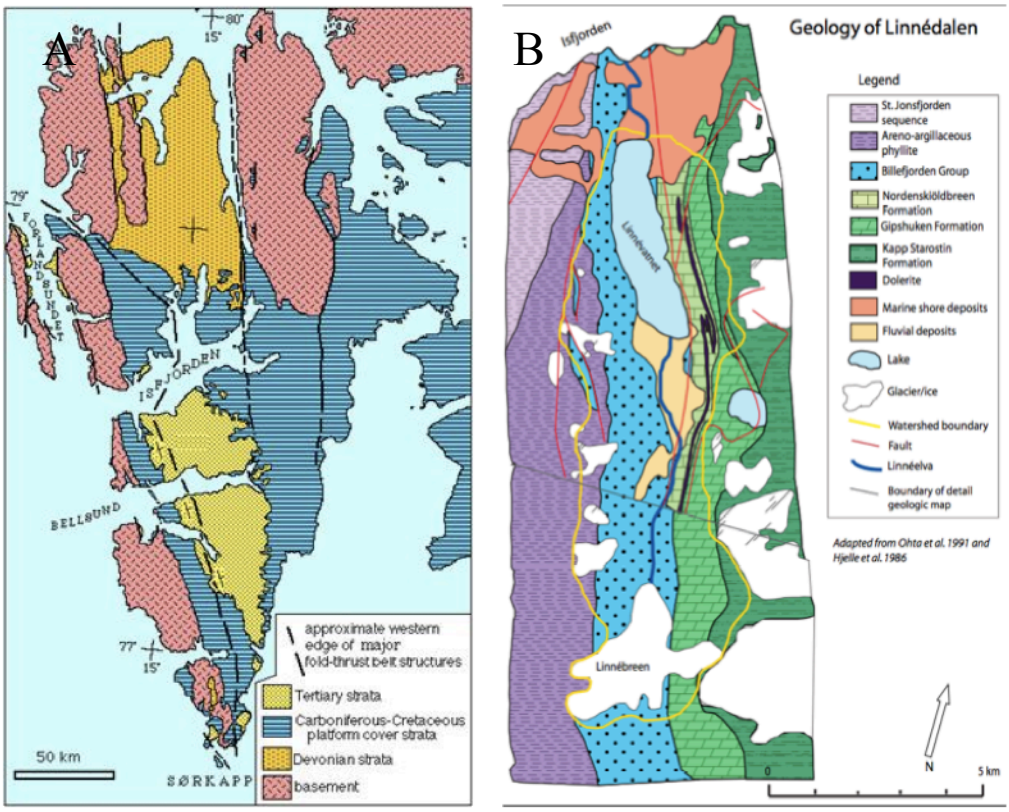

Figure 5: a) General geology of Spitsbergen, Svalbard (Ingólfsson 2004); b) Geologic map of the Linné valley (Perreault 2006)

Lacustrine sediments thicken to the east on the lake bottom: the thickest deposition occurs just to the east of the inlet of Linnéelva (Snyder et al. 1999). Echosounding profiles of the lake bottom show sediment thickening in the topographic lows, especially in the main basin, indicating redistribution of sediment by gravity flows and slumping (Mangerud et al. 1990). The Linné valley is characterized by Precambrian to Ordivician schists and phyllites of the Hecla Hoek Complex in the west, Carboniferous sandstone, coal beds and limestone through the middle of the valley, and folded Tertiary sediments to the east (Figure 5) (Boyum et al. 1978; Snyder et al. 1999).

1.4.2. Study Site: Linné glacier

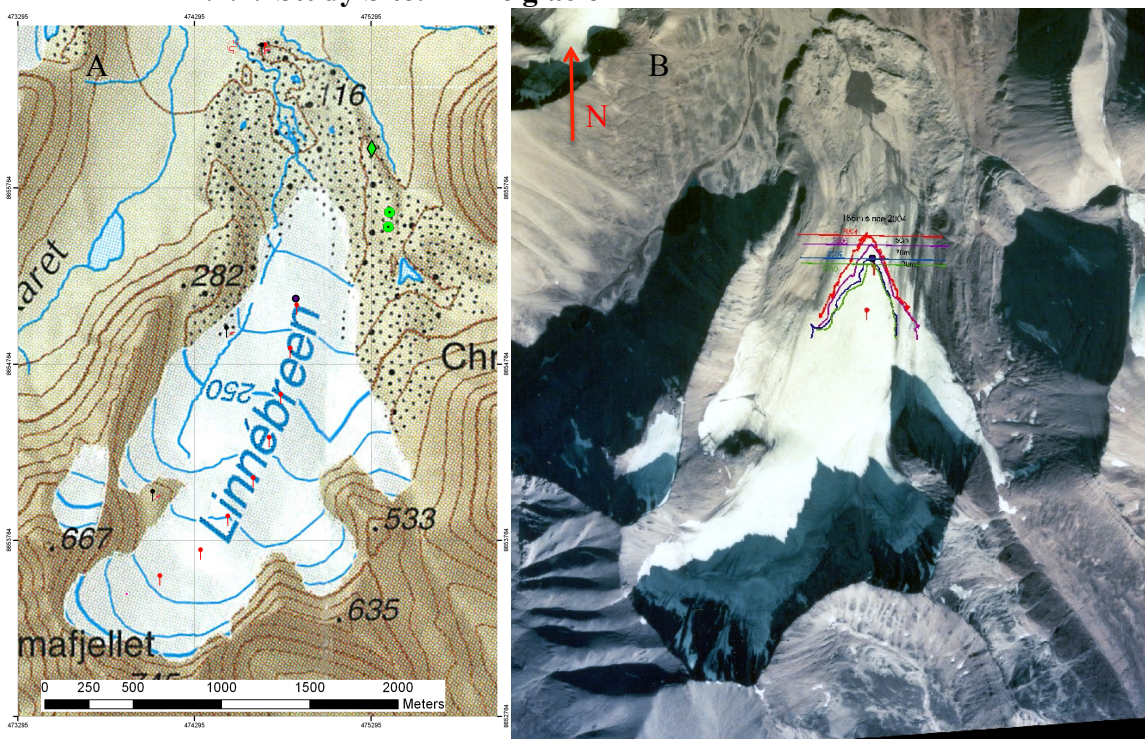

Figure 6: a) Topographic map of the Linné glacier with ablation stakes in red; b) 1995 aerial photo showing the Linné glacier and Little Ice Age moraine with 2004 Terminus in red and 2010 terminus in green. Images courtesy of Norsk Polarinstitutt.

The study site for this project, the Linné glacier, is located at 77°57' north latitude and 13°52' east longitude, at the south end of the Linné valley (Figure 6). The Linné glacier is currently 4 km long and a maximum of 1 km wide with an approximate area of 1.7 km^2 and volume of 0.072 km^3 (Mangerud et al. 1990; Schiff 2004). Helfrich (2007) has characterized the Linné glacier as a polythermal glacier, having zones of both polar and temperate ice. The glacier is in the process of excavating metamorphic phyllites of the Precambrian Hecla Hoek Formation near its headwall as well as Carboniferous limestones, sandstones, and coal seams (Figure 5b). During a climate shift in the Linné valley around 12,300 B.P., the Linné glacier retreated rapidly up the valley to near its present position (Mangerud et al. 1990). Werner

(1993) used lichenometric dating to characterize four periods of glacial stability during the late Holocene at 1500 ya, 1000 ya, 650 ya and most recently during the LIA. Maximum expansion of the Linné glacier during the Holocene occurred during the LIA, evidenced by prominent ice cored moraines and a large moraine complex dated to the LIA (Mangerud et al. 1990; Werner 1993). During the last century, the Linné glacier has been in a state of retreat; a 1936 aerial photo (Figure 4b) shows the glacier abutting the LIA moraine while a 1995 aerial photo (Figure 6b) with terminus positions from 2004 – 2010 shows the glacier retreating upvalley. Glacier area has shrunk by 60% since the 1930s (Matell 2006), which is twice the regional retreat rate over the last century.

1.5. Meltwater and Sediment Production in Glaciated Catchments

Where they occur, glaciers are important components of the hydrologic regime in catchments. The glaciers modify the fluvial system by increasing streamflow volume and, more importantly, they exhibit more pronounced changes in the hydrologic system due to localized meteorological forcings (Hodgkins 1997). Glaciers also moderate the distribution of discharge (and therefore SSC) over the course of the melt season. In Svalbard, approximately 75% of runoff occurs in July and August, though the early season (May – June) is characterized by peak discharge flows from melting of the supraglacial snow (Hodgkins 1997). These early spring peak flows are observed in the Linné valley during mid to late June (Figure 7). During the second half of the melt season (July – August), the supraglacial meltwater store has been exhausted, and the hydraulic regime becomes dependent on climate-induced melting of the glacier, causing a more diurnal discharge pattern (Hodgkins 1997; Hock 2005).

Figure 7: Photographs showing the Linné glacier and upper meltwater channel on June 18th (left) and June 28th (right), notice rapid loss of snowpack over the course of 10 days.

2. Methods

2.1. Suspended Sediment Concentration (SSC)

Two ISCO 6712 water samplers, one at a proximal (Upper) (Figure 8) and one at a distal (Lower) location (Figure 9) from the glacier terminus, were set up to monitor SSC.

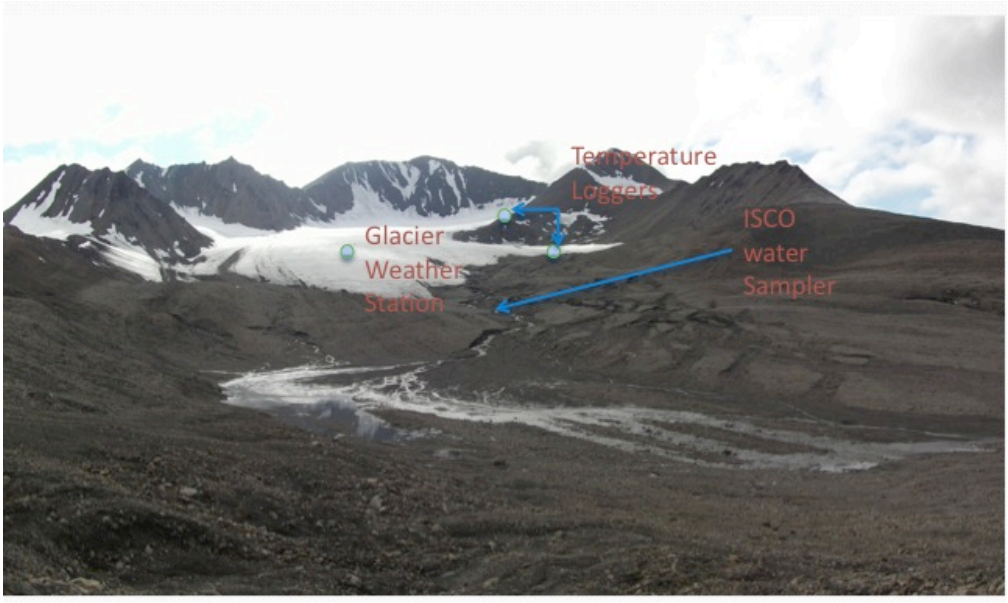

Figure 8: Upper (proximal) sampling site with the Linné glacier in background and meltwater channel in foreground. Note braided nature of the channel below sampling site.

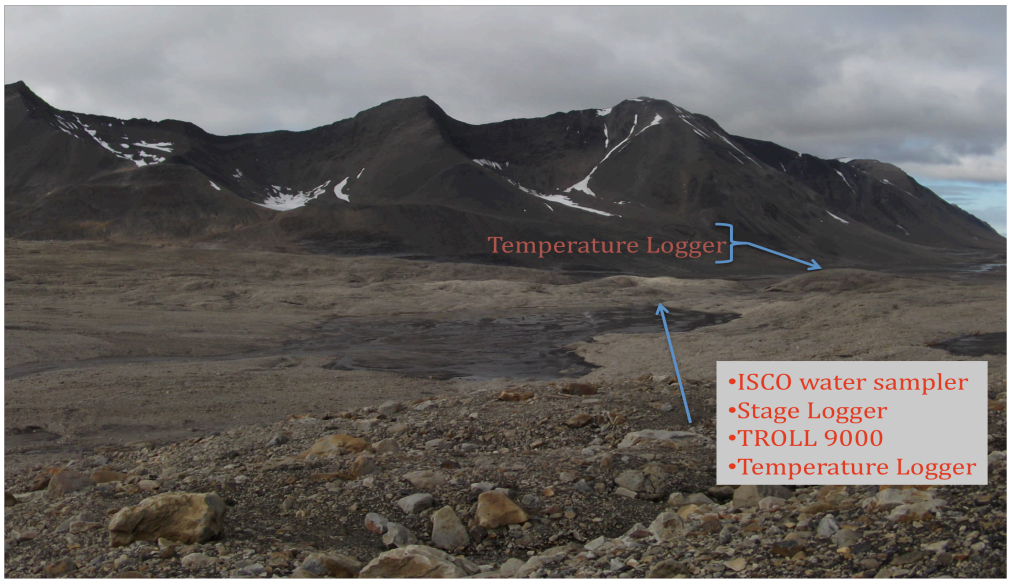

Figure 9: Lower (distal) sampling site on meltwater channel with temperature logger located on LIA moraine in background. Note presence of large braidplain just upstream of sampling site.

The water samplers were powered by 12-volt car batteries connected to portable solar panels that allowed the units to remain in the field for the duration of the field season (Figure 10). The units were programmed to draw a 0.5 L sample every 2 hours from July 21 through August 9. The intake sieve was extended out to the center of the channel and suspended in the middle of the water column with rope (Upper site) or a buoy (Lower site) (Figure 10). The centered position of the intake sieve, both across the channel and in the water column, was chosen to obtain the most accurate SSC samples and avoid clogging of the intake sieve by bedload. However, in such a dynamic environment, it is hard to foresee the effects of extreme conditions. During a high discharge event, a clogged intake sieve at the Upper site caused the loss of 4 samples on the morning of July 30th. A plastic mesh was inserted into the intake to avoid further clogging. After the 24 samples bottles in each ISCO were filled, they were transferred to 0.5 L nalgene sample bottles (Figure 10) and carried back to the field laboratory at Isfjord Radio. A temporary sedimentology laboratory was set up at the station to process the 432

water samples collected during the season. Before filtration, filter papers were cleaned by running water through them to remove any production impurities. The papers were then dried and their mass recorded. Using a gravitational filtration method aided by a portable vacuum pump and 0.45 micron filter paper, each sample was filtered (Figure 10) and then dried in an electric oven at 90˚C for 20-30 minutes. Once dried, the samples were massed and packaged in individual pouches for transport to the United States.

Figure 10: a) Lower sampling site with ISCO water sampler, intake sieve attached to buoy in channel, battery, and solar panel; b) Temporary sediment processing lab at Isfjord Radio station with four gravity filtration units.

2.2. Stream Parameters

2.2.1 Discharge

Discharge measurements are challenging in the glaciofluvial environment of the Linné glacier. In most places, the meltwater channel lacks the width, depth and consistent current required for the area-velocity method. The channel is 1 – 4 m across and has a depth of 10 – 40 cm (Figure 11).

Figure 11: Meltwater channel just upstream of Upper sampling site, showing shallow, and turbulent flow.

As a result of these limiting characteristics, a salt dilution tracer method was employed as described in the USGS Streamflow Manual (Rantz et al. 1983). This method is based on the principle of conservation of mass. A known concentration of salt is injected into the stream and allowed to thoroughly mix; the resulting concentration is measured at a point downstream. The discharge can then be calculated based on measured concentration of the tracer. During each excursion to Linné glacier the discharge of the meltwater channel was measured at approximately 1300. The tracer slug was prepared by dissolving 0.5 kg of NaCl in 4 L of stream water. This slug was injected just below the upper sampling site by pouring the salt mixture across the channel to ensure complete mixing. Approximately 200 meters downstream a student was positioned in the middle of the channel, submersing a TROLL 9500 water quality-monitoring instrument. The TROLL recorded the electrical conductivity (microSiemens/sec) of the meltwater, which showed a significant spike as the slug of concentrated Na^+ and Cl^- ions flowed by (Figure 12).

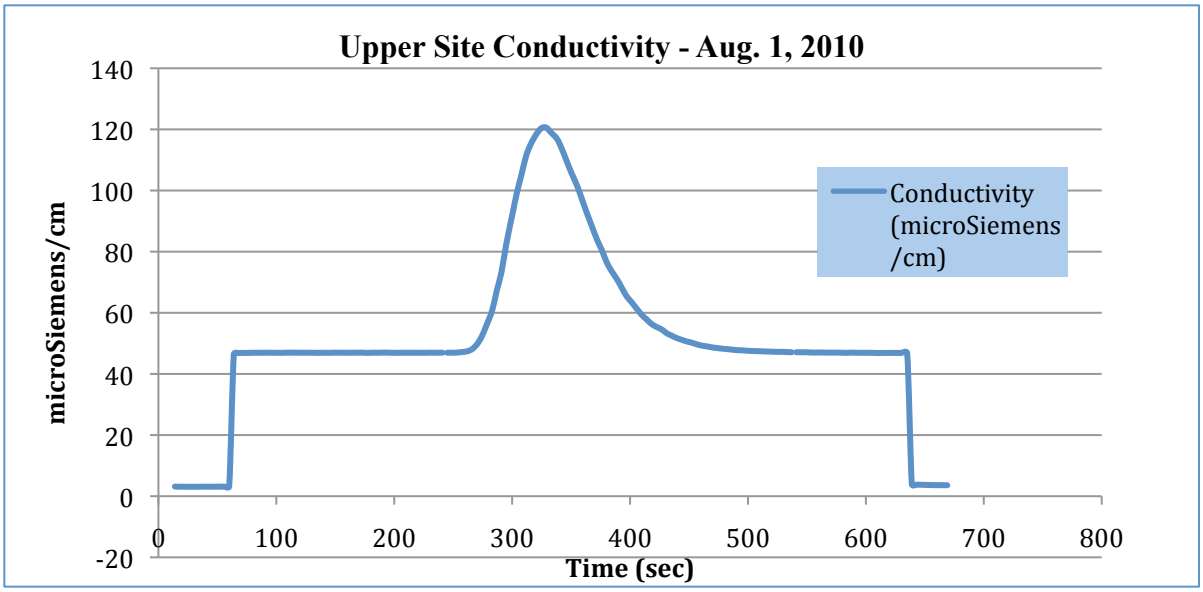

Figure 12: Graph showing spike in conductivity from injection of salt-tracer slug during discharge measurement.

The conductivity is then converted to a concentration of NaCl/L by multiplying by the experimentally derived conversion of 0.51 (NaCl/L)/ (microSiemens/sec) (Apps 2002). Utilizing the principle of conservation of mass, the discharge is then calculated using:

$$Q = \frac{V_1 C_1}{\int_0^\infty (C - C_b) dt},$$

Where Q is the discharge of the stream, V_1 is the volume of tracer solution injected, C_1 is the concentration of the tracer solution, C is the measured concentration, C_b is the background concentration of the stream, and t is time (Rantz et al. 1983).

Sources of error involved with this method are the loss and incomplete mixing of the tracer. Loss of the tracer due to chemical reaction is negligible and only becomes significant over extremely long reaches of channel. Loss of tracer to sorption is dependent on the texture of the streambed and length of reach (Rantz et al. 1983). The minimal distance of the reach reduces the loss of tracer to both chemical reaction and

sorption. The short reach of channel also limits the influence of hyporheic flow into the channel from surrounding substrate. Incomplete mixing of the tracer would give a higher than expected concentration measurement and is usually due to incomplete mixing laterally rather that vertically. Introducing the tracer slug evenly across the channel, as well as the small and highly turbulent nature of the channel itself, has minimized this source of error.

Through the salt dilution tracer method, a number of instantaneous discharge measurements were obtained over the field season. In order to complement these measurements, a HOBOware level logger recorded stage at the lower site throughout the season (Figure 10a). The logger was a sealed pressure transducer, which meant the readings had to be corrected for atmospheric pressure using barometric pressure readings from the main weather station downvalley. A stage – discharge rating curve (Figure 13) was then developed and used to calculated a discharge record for the duration of the field season.

Unfortunately, it was impossible to anchor the stage logger at the Upper site due to the rocky channel bottom and dynamic channel behavior, which would have led to erroneous measurements. Therefore, the logger was located at the lower site, though the discharge

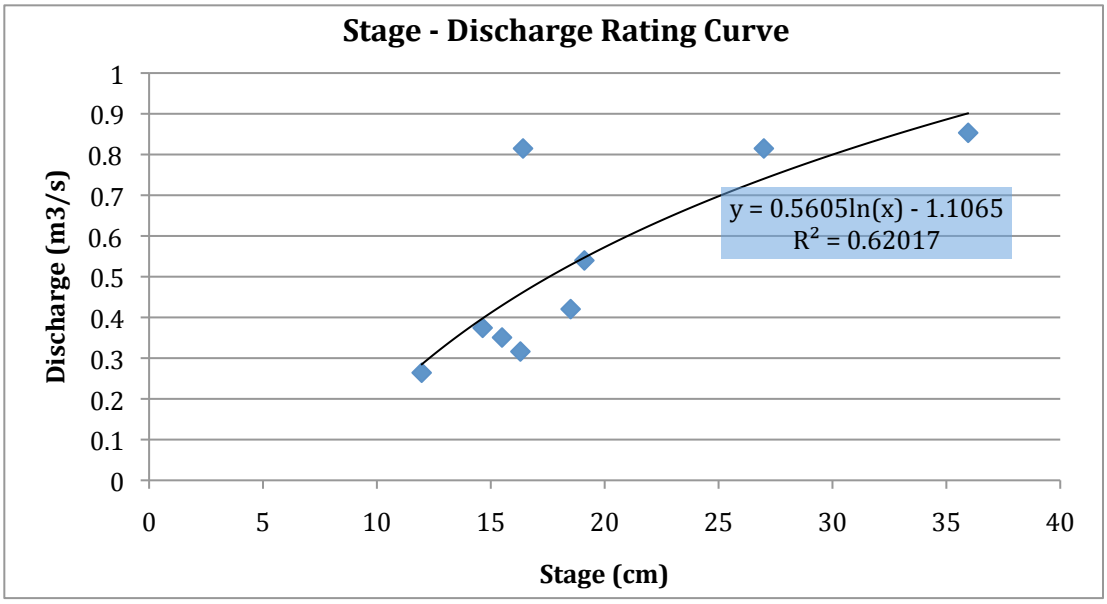

Figure 13: Stage-discharge rating curve developed using instantaneous discharge measurements and season-long stage record in order to calculate discharge record for the field season.

measurements were taken approximately 400 m upstream. This distance and the existence of a small tributary (< 0.01 m^3/s), lowered the R^2 value of the rating curve, but the relationship is still probably characteristic of the flow emanating from the glacier.

2.2.2 Temperature

A HOBOware water temperature instrument attached to a rock anchor in the middle of the channel recorded temperature of the meltwater from July 20 to August 9, 2010. The data was uploaded after the field season and the logger replaced in the channel to continue data logging for next season.

2.2.3 Turbidity

A TROLL 9000 water quality monitor attached to a post driven into the channel bottom at the Lower site (Figure 10) was responsible for gathering turbidity readings for the field season (July 20 – August 9, 2010). This instrument had to be installed at the Lower site in order to obtain accurate data and to avoid damage to the

instrument. Turbidity data was recorded in NTUs every minute during the field season and averaged over 30 minute intervals in order to consolidate data to a manageable size.

2.3. Meteorological Data

Meteorological data was collected at a number of locations in the Linné Valley during the summer of 2010. The glacier weather station, located at ablation stake #3, recorded air temperature, precipitation, and solar radiation (Figure 14a). Two other temperature loggers located on the northern edge of the glacier, one near the toe and one near the cirque headwall, also recorded air temperature (Figure 14b). A third air temperature logger was installed on the LIA moraine. Farther downvalley, the main weather station recorded air and ground temperature, as well as wind direction, precipitation, and barometric pressure (Figure 14c).

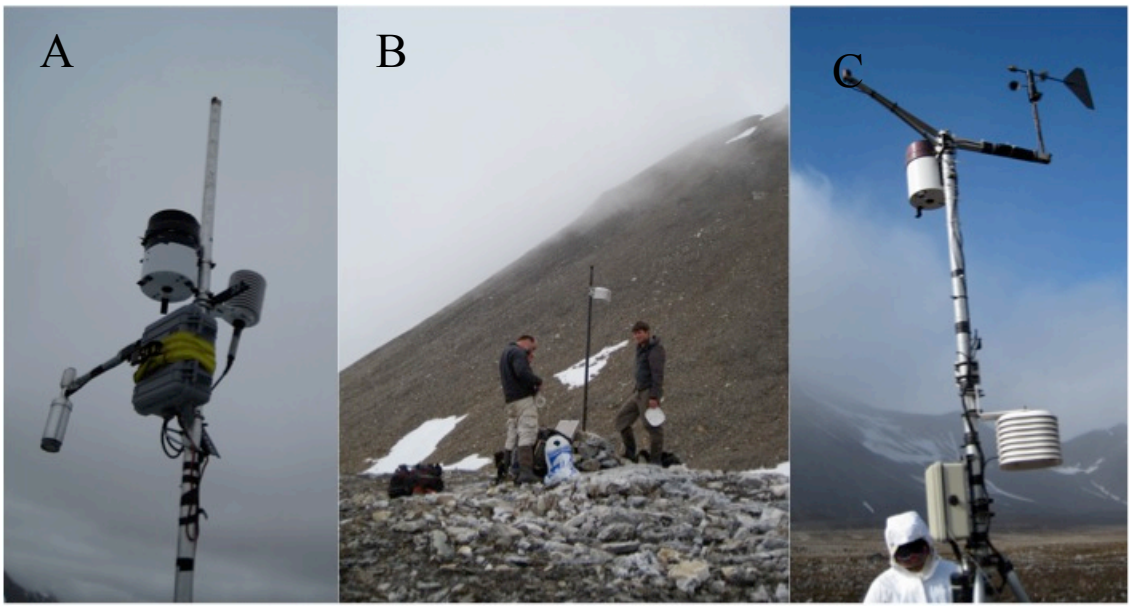

Figure 14:a) Ablation stake #3 weather station on glacier; b) Air temperature logger near cirque headwall; c) Main Linné valley weather station located further downvalley.

2.4. Glacial Surface Lowering

Glacial surface lowering data was obtained by regularly monitoring the 8 ablation stakes located on the glacier (Figure 6a). This data was collected and processed by Terra Hittson who was monitoring the dynamics of the surficial processes on Linné glacier during the field season.

Glacier ablation values collected during the field season were extrapolated over an aerial photo of Linné glacier in GIS. The resulting raster containing extrapolated ablation values in meter square plots was then used to calculate a volume of ice lost during the monitoring period.

2.5. Grain Size Analysis

Grain size analysis of selected SSC sediment samples was completed at Bates College on January 6th, 2010 with the assistance of Svalbard REU advisor Mike Retelle. Each sample was scraped from its pouch and filter paper and placed in a 47-mL Oak Ridge centrifuge tube. The samples were scraped from their filter papers rather than washed from the filter paper using a solvent. However, only a thin film of particles remained adhered to the paper. The samples where then covered with 30 mL of dispersant solution (0.7 g/L sodium metaphosphate) to promote disaggregation. Each sample was shaken for one minute and then sonicated (using a Fisher Scientific 60 Sonic Dismembrator) for one minute to deflocculate any fine particle clumps that remained aggregated.

The Beckman Coulter LS13 320 Particle Size Analyzer (PSA), determines particle size by single wavelength laser diffraction. A laser beam is shot through a chamber of the particle solution and the subsequent diffraction pattern is measured by

photo detectors and converted into grain sizes. This PSA can measure a range of particles from 0.4 to 2000 microns. Each sample solution was shaken and sonicated for one minute again before being introduced into the PSA. Each sample went through three, one-minute grain sizing tests and the average particle size was used in the results.

3. Results

3.1. Suspended Sediment Concentration (SSC)

Collected SSC data from July 21st through August 9th are presented in Figure 15.

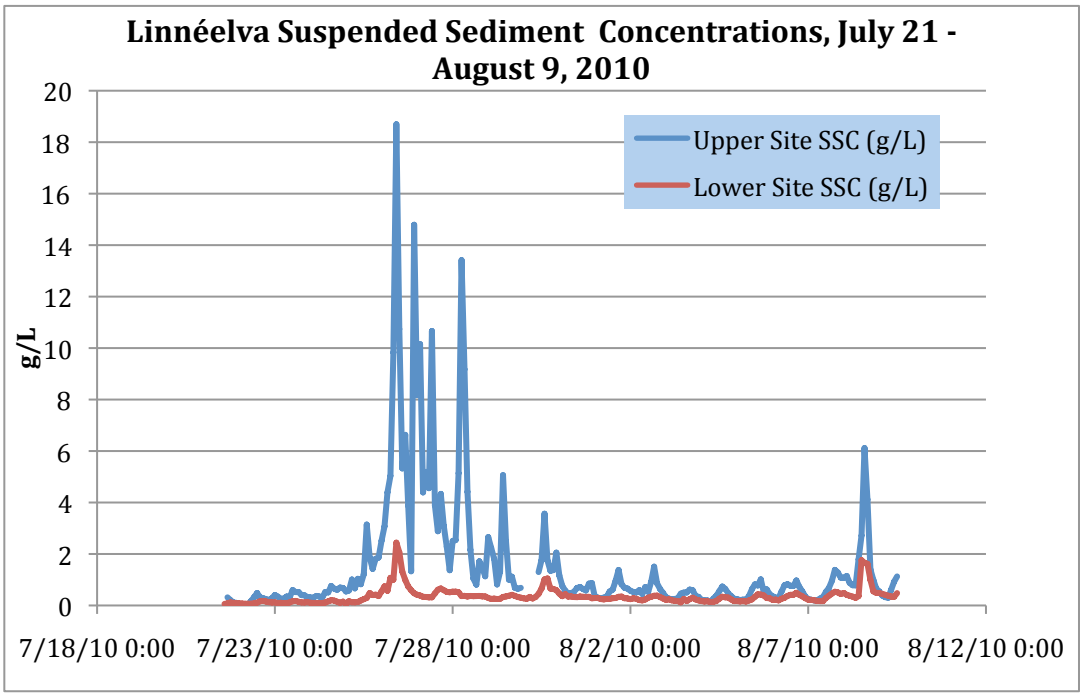

Figure 15: Suspended Sediment Concentration (SSC) data collected from Upper (blue) and Lower (red) sampling sites during the field season.

The Upper and Lower sampling sites show fluctuations in SSC that match over time but not in magnitude. Sediment concentrations measured at the Upper site were generally higher than those of the Lower site levels and upward of nine times the concentration during peak events. The decreased magnitude and variability of the Lower site can be attributed to its greater distance from the glacier, the decrease in gradient of the channel and the presence of a small braid plain that allows for the settling of sediment from the water column before reaching the sampling site. Three major SSC peaks are evident in Figure 15, occurring on July 26th and 30th, and August 8th. The lowest recorded

SSC for both sampling sites occurred at 02:00 on July 22nd, with the Upper site measuring 0.079 g/L and the Lower site measuring 0.074 g/L. Diurnal patterning is also apparent in the cyclical nature of the measurements from August 1 – 8. The absence of recorded data from 00:00 to 08:00 on July 30th is the result of a clogged intake filter on the ISCO water sampler after a particularly high discharge event.

3.2. Suspended Sediment Load

Based on calculations using SSC and discharge, Upper site sediment yield averaged 75 metric tons per day for a total of 1437 metric tons for the study period, while the Lower site averaged approximately 17 metric tons per day and a total of 318 metric tons of total sediment yield (Figure 16).

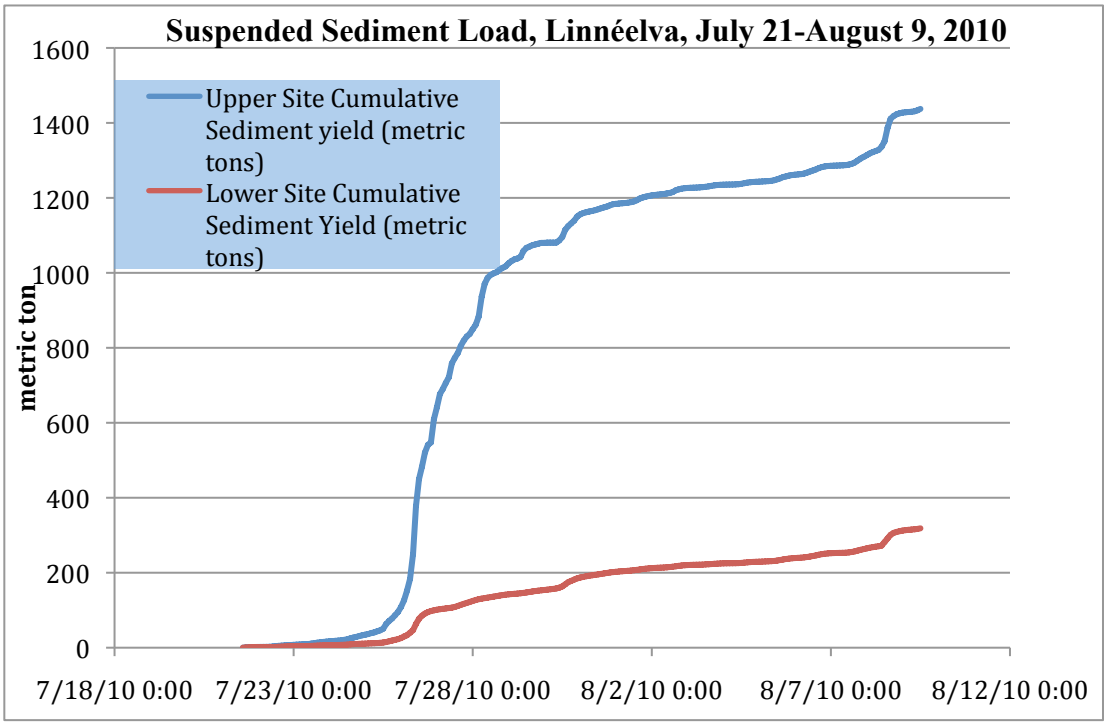

Figure 16: Cumulative sediment yields. Note large difference between proximal (Upper) and distal (Lower) sampling site yields.

3.3. Stream Parameter - Discharge

The hydrograph developed from the stage – discharge rating curve showed marked variability (Figure 17). Discharge data is available from July 7 – August 9, 2010.

The maximum discharge of 0.97 m^3/s occurred at 10:00 on July 26th and the lowest recorded discharge of 0.06 m^3/s occurred at 05:30 on August 4th. Diurnal pattering presents throughout the field season, especially from 06:00 on August 1st to 03:00 on August 6th.

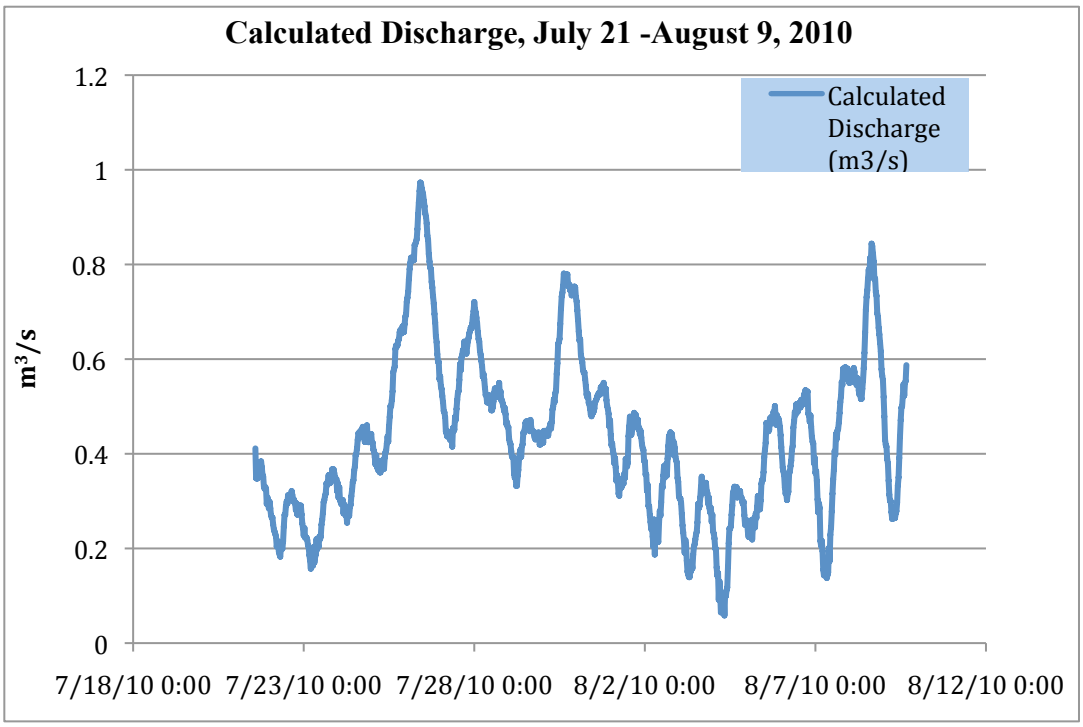

Figure 17: Discharge calculated from stage record for field season.

3.4. Stream Parameter – Temperature

The HOBOware water temperature device measuring the channel temperature at the Lower sampling site recorded water temperature throughout the field season (Figure 18). The maximum temperature (recorded on July 22 at 13:30) was 16.85°C and the minimum (recorded on August 4 at 02:30) was 1.79°C. The temperature fluctuated on a daily basis, with highs of ~4.5°C occurring between 13:00-15:00. Daily low temperatures of ~2.5°C were recorded between 02:00-03:00. Variations in this record are most noticeable on July 26 and August 8, when the channel temperature remained around 3°C, instead of regular temperature highs and lows for those days.

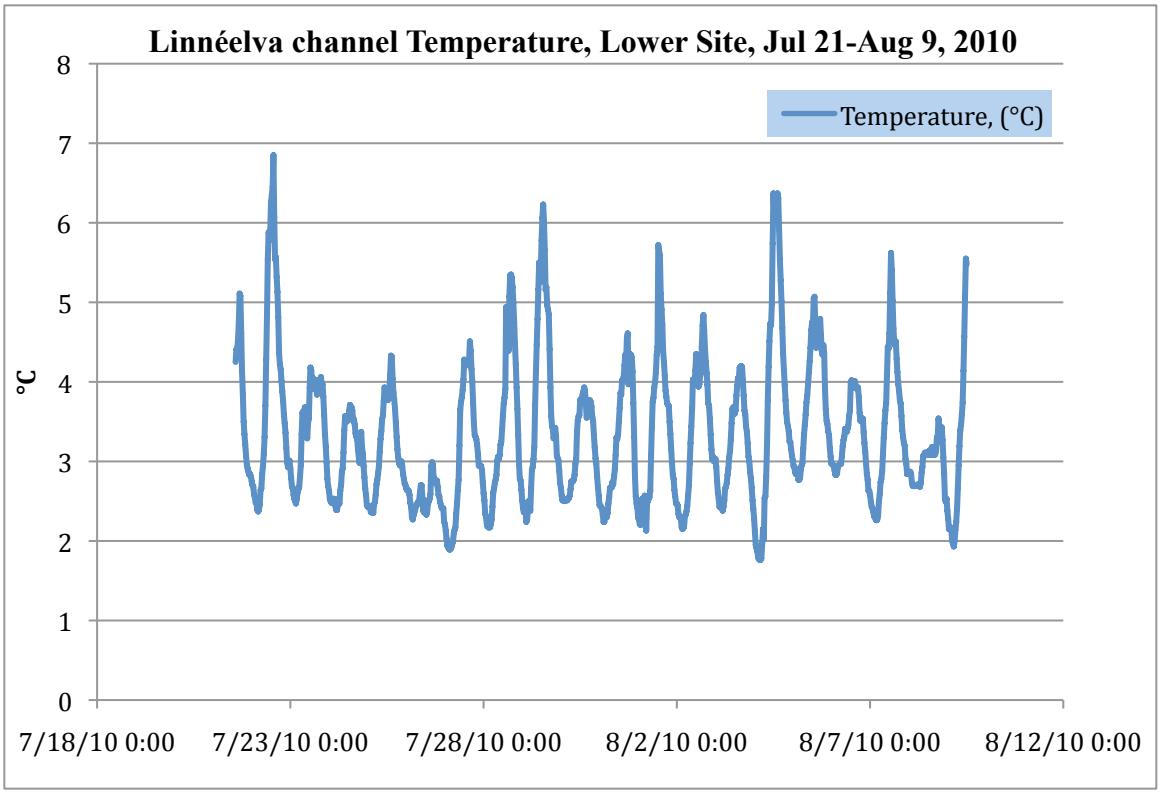

Figure 18: Water temperature from lower sampling site over duration of field season.

3.5. Stream Parameter – Turbidity

The turbidity (NTU) data was collected by the TROLL water quality device at the Lower Sampling site and averaged to 30-minute intervals (Figure 19). The maximum turbidity measured was 2390.4 NTU and occurred on July 26 at 08:00, while the minimum turbidity was 124.9 NTU and occurred on July 26 at 08:00. Three prominent spikes occurred over the course of the field season, on July 26th-27th, July 30th, and August 8th, the same days of above average discharge in the meltwater channel. Outside of the three high turbidity events, the season was dominated by a repeating cycle of highs averaging 600 NTU and lows averaging 320 NTU occurring at approximately 11:00 and 20:00 respectively daily.

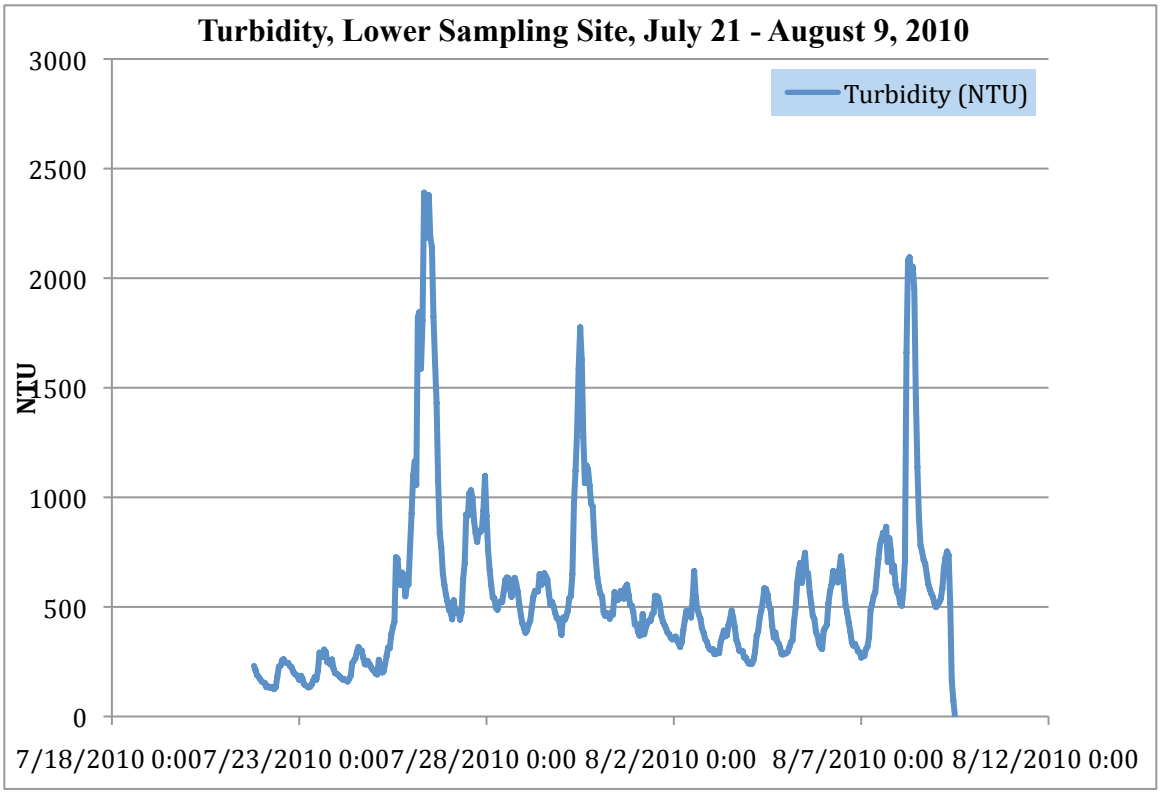

Figure 19: Graph of turbidity recorded at Lower sampling site; note three prominent peaks in turbidity.

3.6. Meteorological Data – Precipitation

Overall precipitation accumulation totaled 71.6 mm over the 19-day field season, arriving almost entirely as rain. Three main precipitation events (Figure 20) were responsible for the majority of accumulation, the largest (30.8 mm) occurring on July 26th. The other events occurred on July 30th and August 8th, accumulating 10.4 mm and 17.4 mm respectively.

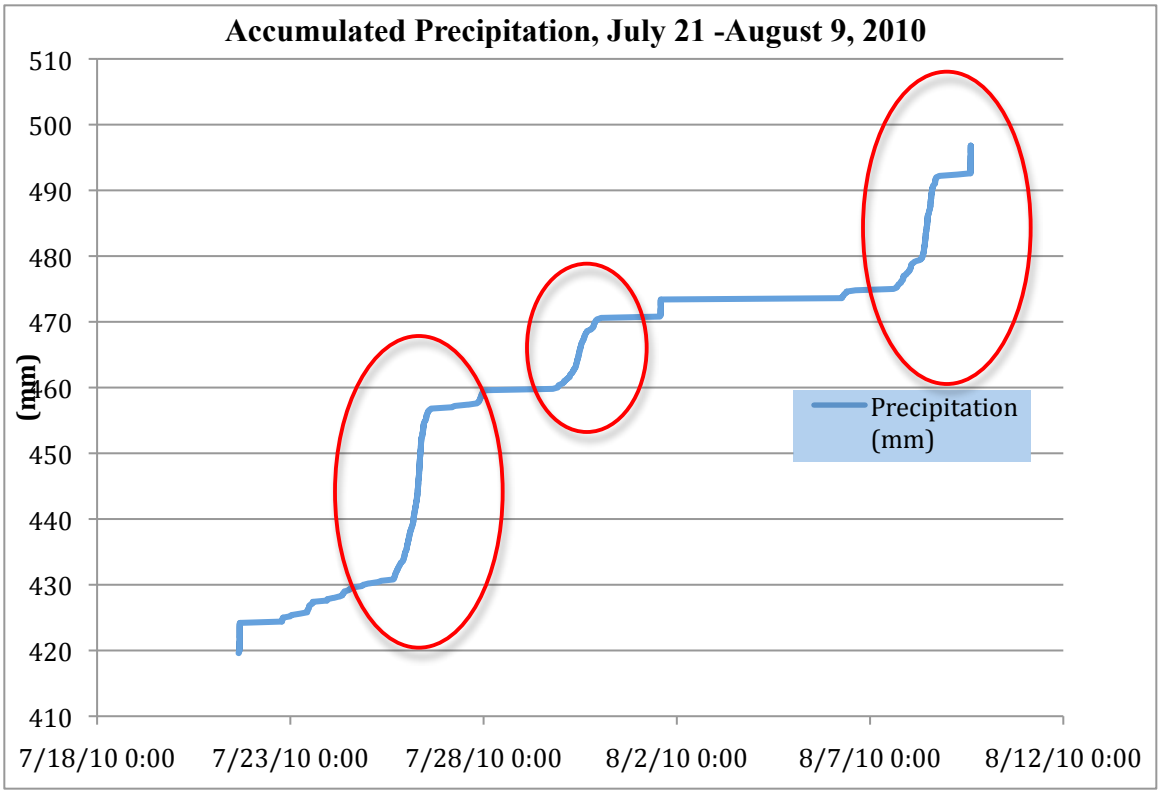

Figure 20: Graph of accumulated precipitation on the Linné glacier, with a total of 76 mm and three major rain events.

3.7. Meteorological Data – Air Temperature

Ambient air temperature in and around the meltwater channel during the field season averaged 4.4°C. The maximum temperature recorded was 6.8°C on July 28th, while the minimum was -0.647°C on August 4th. On average, daily highs were between 5-6°C and lows between 3-4°C. The fluctuations in temperature generally follow a pattern of rising and falling temperature over a 24 hour period, but the highs and lows occurred at all times during that period (Figure 21). The warmest part of the day occurred anywhere from 06:00 to 18:30, with the coolest part of the day occurring with the same variability.

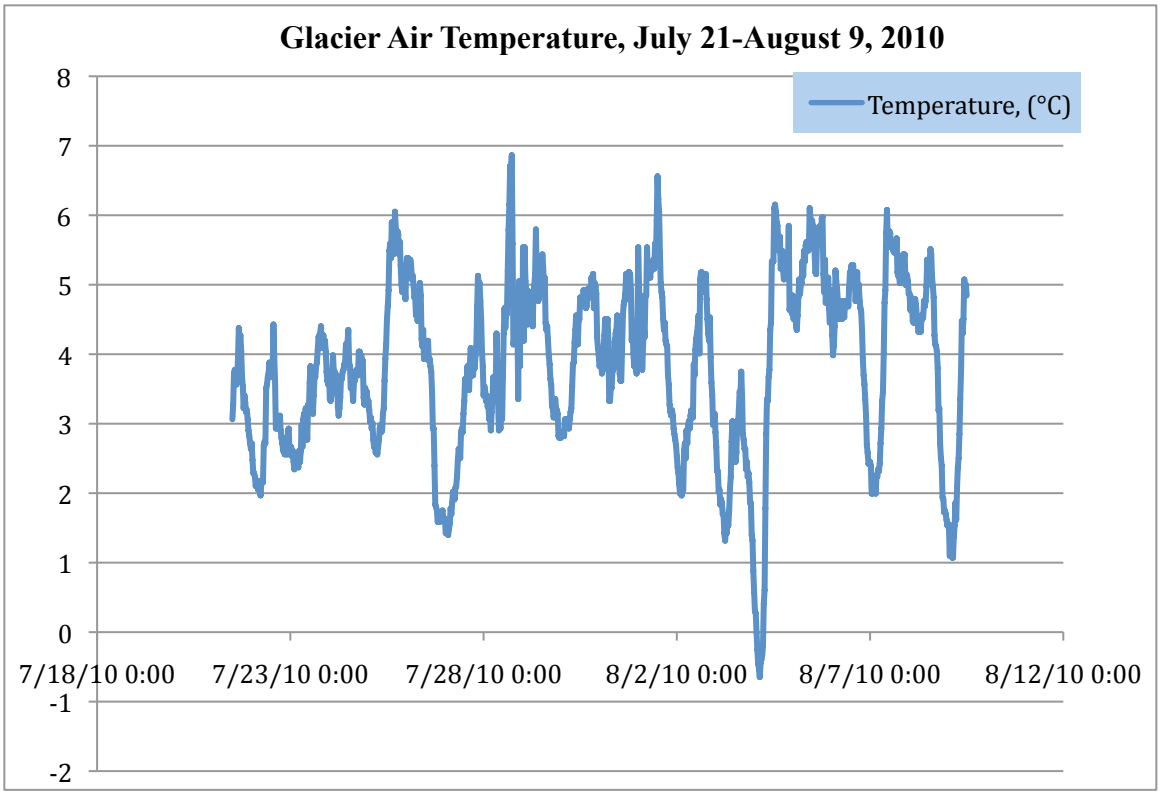

Figure 21: Graph of air temperature taken at ablation stake #3 weather station.

3.8. Meteorological Data – Solar Radiation

Due to the high latitude of the research site, the area was experiencing 24 hours of daylight during the field season. Except during times of cloud cover and when the sun dipped below the headwall ridge, the glacier and glaciofluvial system experienced fairly constant solar radiation (Figure 22). However, also because of the high latitude, the angle of incidence from the sun was quite low, reducing the intensity of the solar energy on the glacier surface. The maximum recorded intensity of 99200.7 lx occurred on August 2nd at 15:00, while the lowest was 516.7 lx on August 8th, at 00:00. Daily, the intensity fluctuated roughly between 45000 and 3500 lx, with the high occurring around 11:00 and the low occurring around 22:00 when the sun was lowest in the sky.

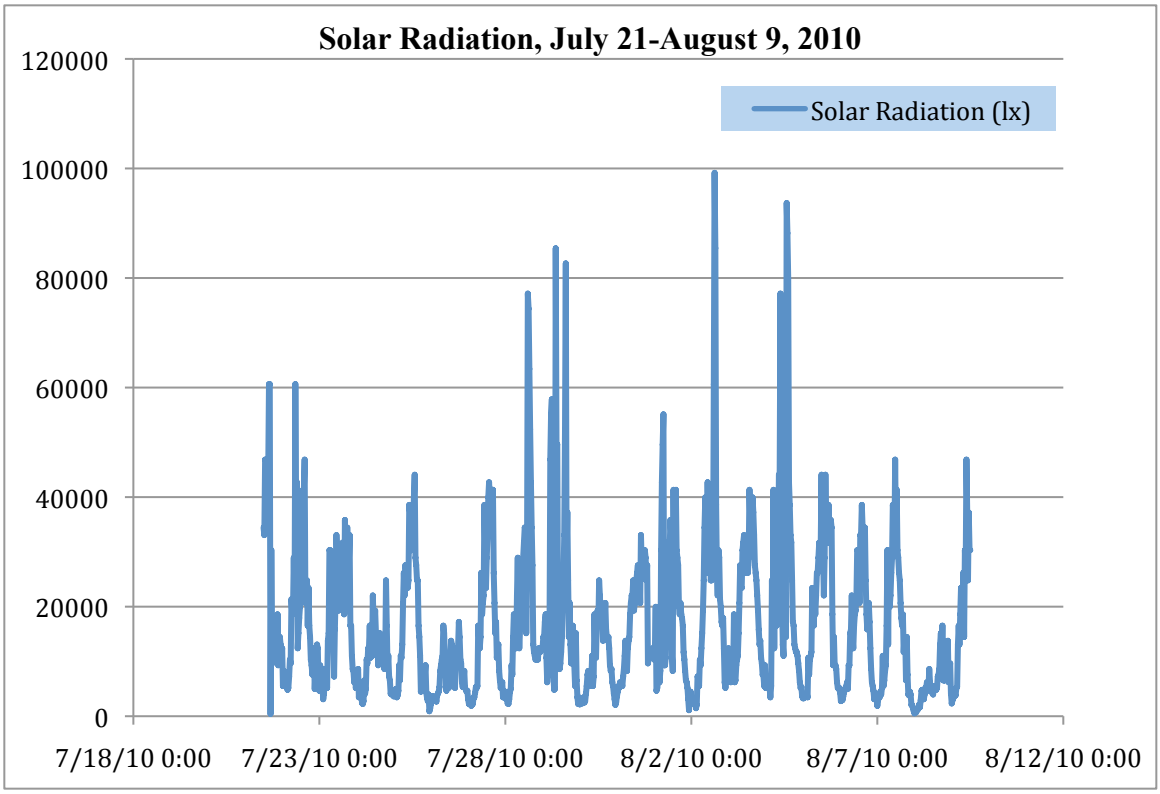

Figure 22: Solar radiation recorded in Lx from glacier Ablation Stake #3.

3.9. Glacier Ablation

Measurements from the 8 ablation stakes running up the centerline of the glacier (Figure 24) showed an average surface lowering of the glacier of 40.4 cm over the 11 days of measurement (Figure 23). Maximum ablation occurred closest to the toe of the glacier at ablation stake #1, where the surface lowered a total of 52.2 cm. Minimum ablation occurred midway up the glacier at stake #4, with an ablation value of only 31 cm. As shown by Figure 23, surface melting rates were highest between July 22 – 28. Lower melting rates occurred before and after this peak, as well as increasing near the end of the study period. Periods of increased surface lowering coincide with the major precipitation accumulation events of the field season (July 23-28), while the lower rates of ablation in the beginning and middle of the study period coincide with lower amounts of precipitation.

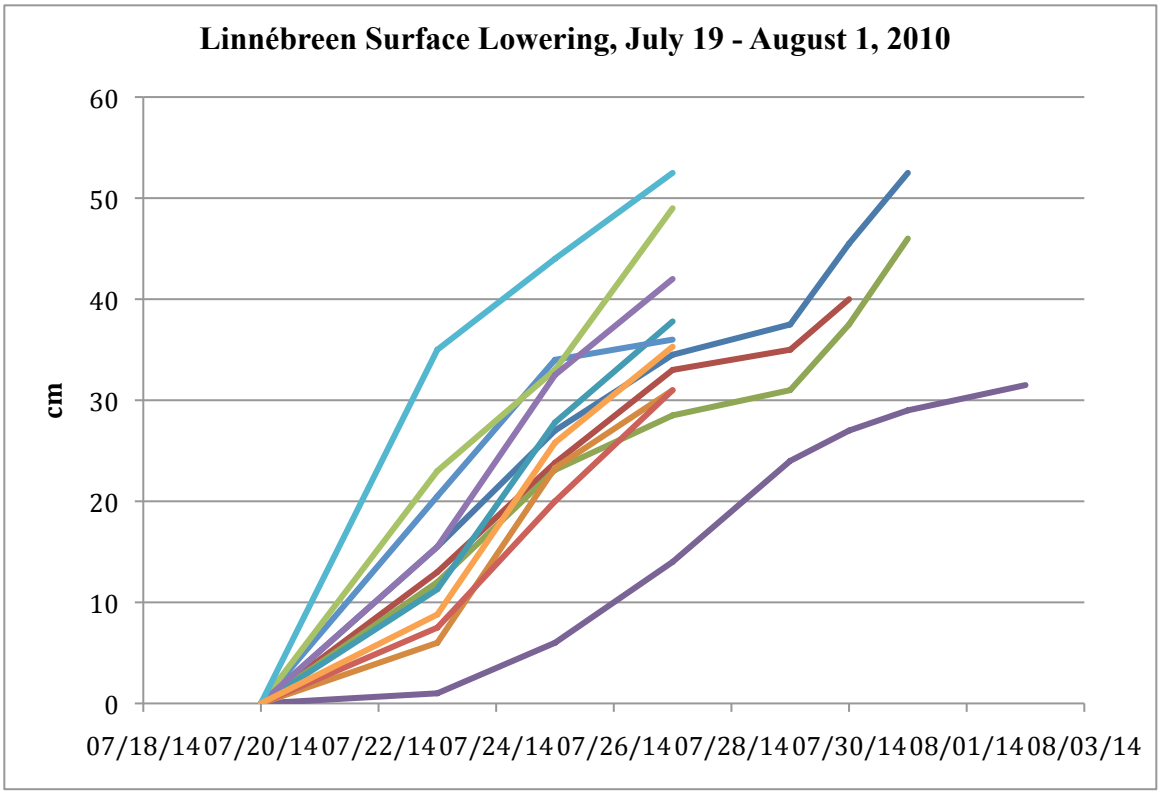

Figure 23: Glacier ablation values for ablation stakes (new and old).

Analysis and computation of ablation data in GIS produced a rough estimate of the volume of ice lost over the course of the 11 day study period and also a graph (Figure 24) showing the variability of melting intensities over the glacier surface. Computation of extrapolated surface lowering values gave a volume of ice lost of about 758,000 m^3, an average of roughly 37,000 m^3 per day. Figure 24 also shows that melting was most intense near the toe and head of the glacier, while the least amount of melting occurred on the steeply sloped section at ablation stakes #2-#4.

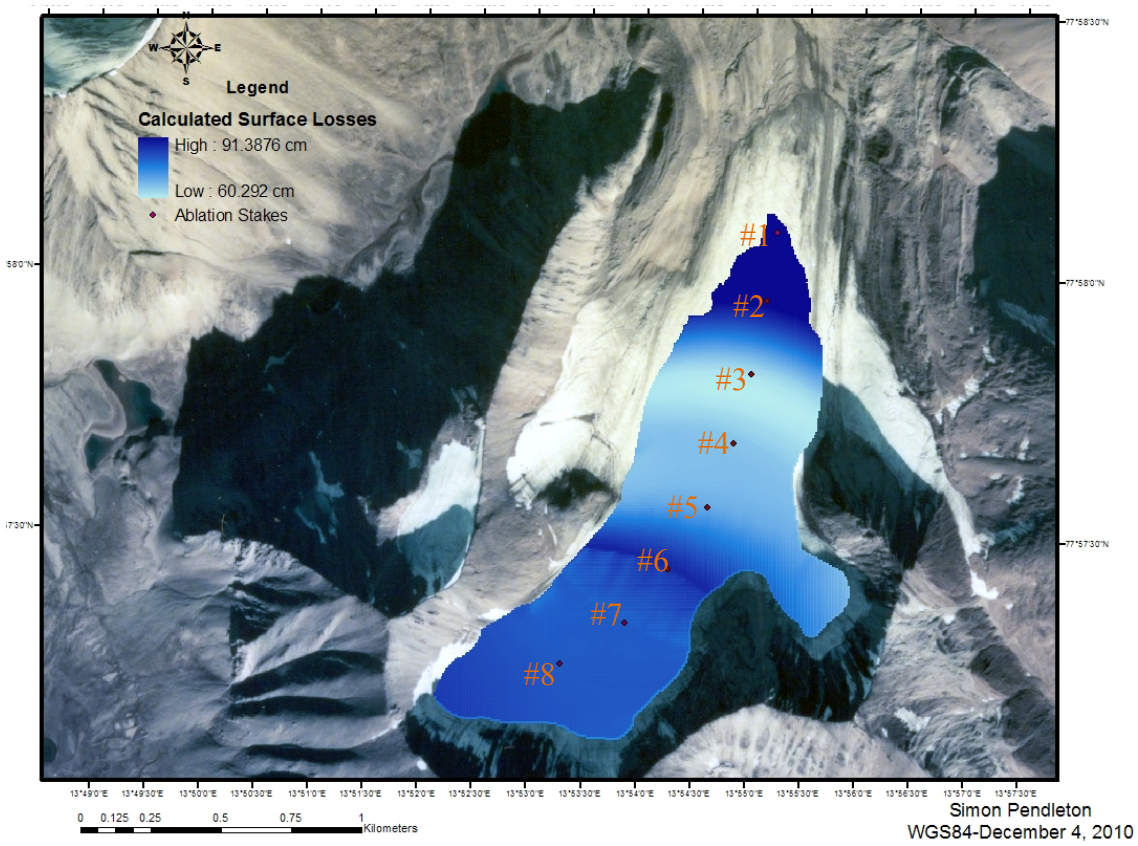

Figure 24: Map of the Linné glacier showing variations in ablation intensity; note high ablation values on the toe and head of the glacier, but lower ablation values on the middle, steeply sloped section. Adapted from Norsk Polarinstituit aerial photo.

3.10. Grain Size Analysis

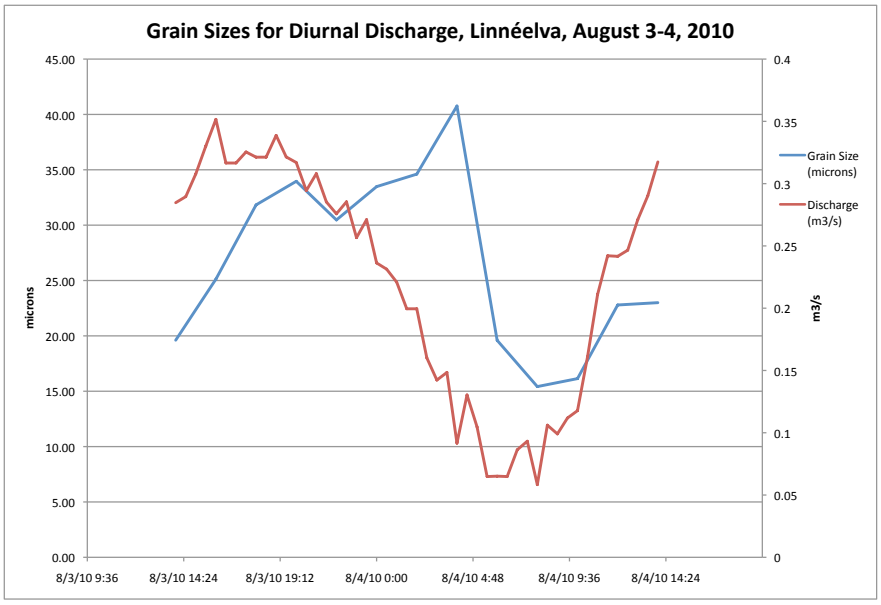

Figure 25: Grain size variation during a diurnal discharge cycle, August 3-4, 2010.

Grain size analysis for a diurnal cycle of Linnéelva, on August 3-4 is shown in Figure 25. The graph indicates that the mean sediment size increased from 20 microns on August 3rd until peaking at 04:00 on August 8th, before returning to the 20 micron size 24 hours later.

The high discharge event on July 25-26 transported grain sizes between 26 and 853 microns during the time discharge was increasing. Figure 26 shows the staggered

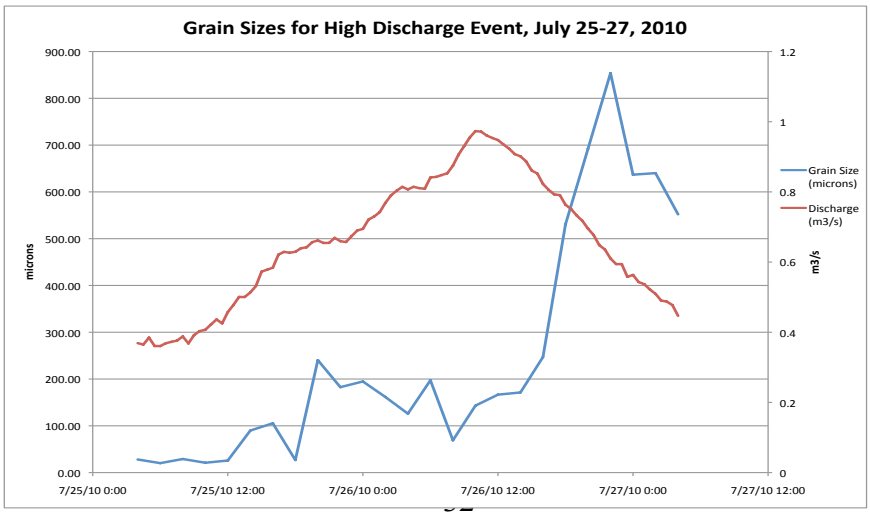

Figure 26: Grain size variation for a high discharge event, July 25-27, 2010.

increase in grain size over the course of the event until peaking at 22:00 on July 26th, before trending downward with decreasing discharge.

Analysis of the grains from the low discharge event on August 4-5 shows the smallest range of size of grains: from 15 to 33 microns (Figure 27).

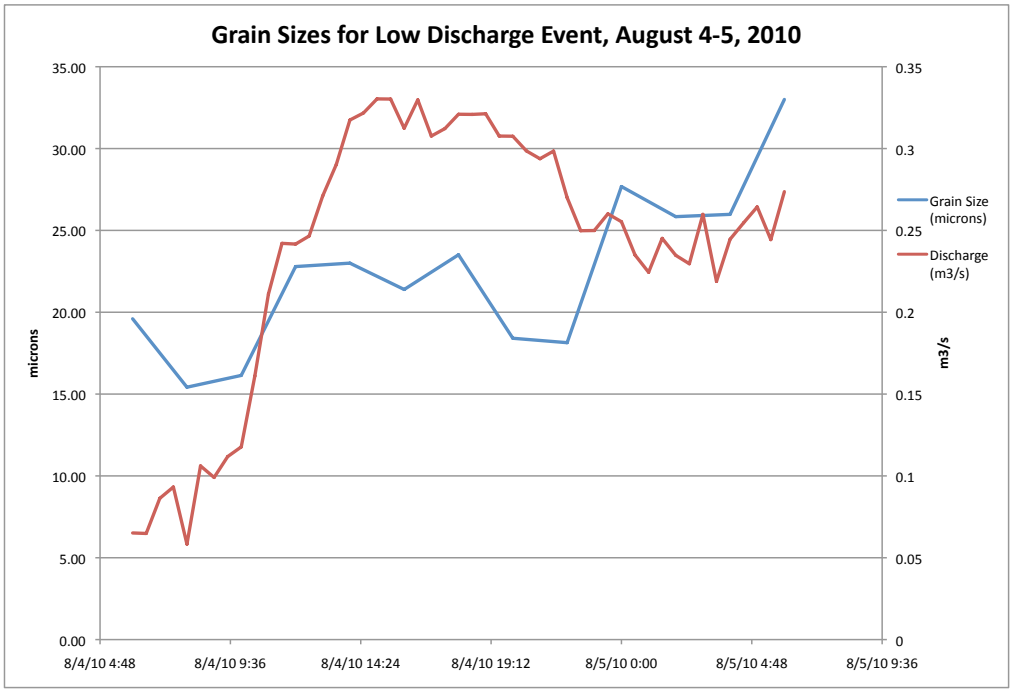

Figure 27: Grain size variation during low discharge event, note limited range of grain sizes relative to high and diurnal grain size analysis.

4. Discussion

The goal of this project is to determine the climatic controls on sediment production from Linné glacier and to establish the parameters under which the glaciofluvial system processes the sediment produced by the glacier. In order to establish how meteorological conditions influence sediment production, it is important to understand the primary parameters of the glaciofluvial environment that are controlling SSC and then determine what climatic conditions responsible. In this way, the links between sediment production and various weather conditions can be established. Determination of the processes controlling SSC and how the glacier is responsible for those processes will ultimately link sediment production to meteorological conditions.

4.1. SSC and Discharge

As expected, SSC is shown to be dependent on discharge. As the discharge and velocity of the meltwater stream increase, the amount of suspended sediment increases as well. The amount and timing of peak SSC events during the study period is directly related to discharge, as shown in Figure 28. Both SSC and discharge exhibit matching peaks during the major precipitation events occurring on July 26th and 30th and August 8th. As discharge begins to enter a diurnal pattern starting on August 1st, SSC also begins to show matching diurnal characteristics. Differences in SSC and amount of sediment entering the system versus leaving the system will be discussed in a later section.

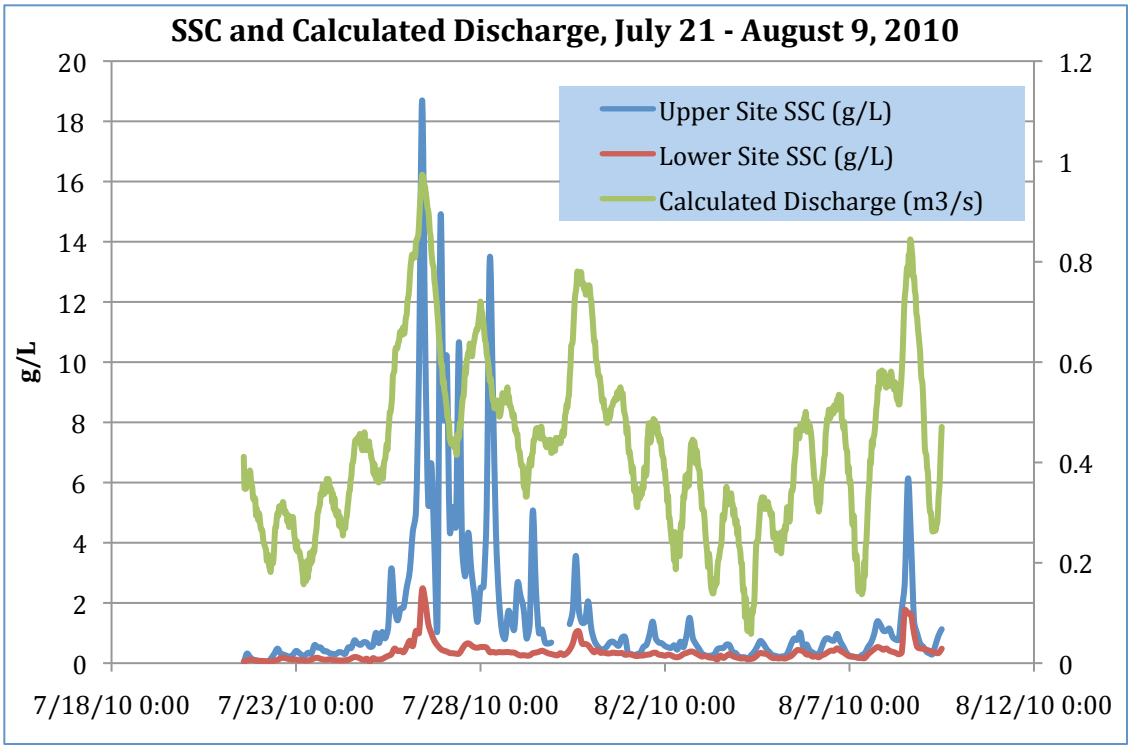

Figure 28: Graph of SSC and discharge, note correlating high discharge and high SSC events, as well as low, diurnal discharge and low diurnal SSC.

4.2. Discharge and Glacier Melt

In a non-glacierized catchment, precipitation and groundwater will have the most pronounced influence on discharge. In the case of the Linné glacier and the proximal glaciofluvial environment, glacier melt is the main driver of discharge. Therefore, the climatic condition causing the most glacial melt will also be the main control of discharge. Since it has been observed that discharge is the main control of SSC, it then follows that the meteorological conditions causing the most glacial melt will also have the greatest influence on sediment production.

Work by Stewart (2007) and Helfrich (2007) on Linné glacier during the summer of 2006 found that precipitation was the cause of the most glacier surface melt. Observations by Hittson (2010) during the summer field season also indicated precipitation was more important than solar radiation and air temperature as a driver of

glacial surface melt. Figure 29 shows the correlation between times of precipitation accumulation and high rates of glacier melt, as well as lower rates occurring during times of little or no precipitation accumulation. Unfortunately, due to the minimal number of ablation observations (7) versus the high sampling rate of precipitation, the correlation between glacial melt and precipitation appears somewhat offset, but the general trend of low ablation rates with low precipitation and higher ablation rates with higher precipitation is still apparent.

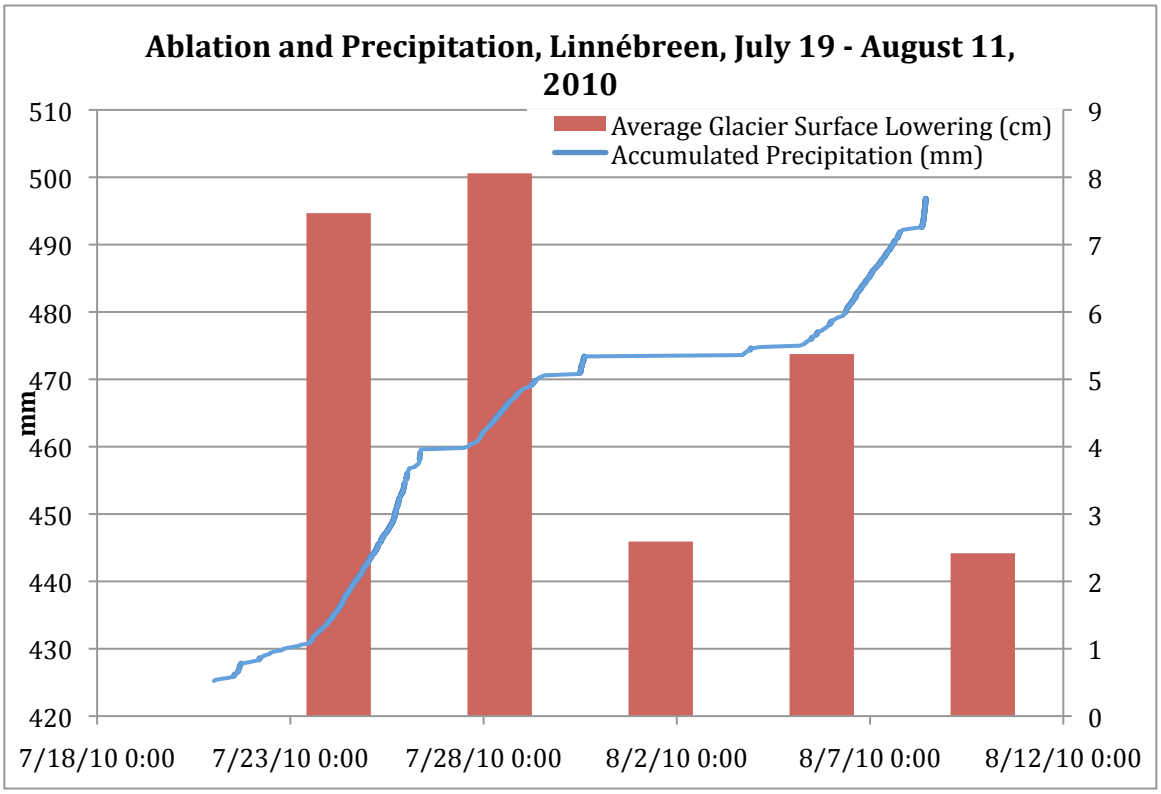

Figure 29: Graph of glacial ablation values and precipitation from July 19-August 1, 2010.

4.3. Discharge and Precipitation

Understanding that in the Linné glacier setting, glacial melt has the largest influence on discharge, and having seen that precipitation is the main driver of glacial melt, it follows that precipitation is then the main driver of discharge. The catchment is highly responsive to precipitation events, as evidenced by the minimal lag time of the hydrograph, which is on average less than an hour (Figure 30). This is due to the small catchment size (<8 km^2) and the accelerated melting of the glacier surface caused by rain (Hittson 2010).

Figure 30 clearly shows the direct effect that precipitation has on discharge by the correlation between the three prominent precipitation events with the three peaks in discharge. During the period from July 30th to August 4th, there was little precipitation, and the discharge record began to decline and enters a pattern of diurnal cycling. Without the influence of precipitation, discharge must be controlled by another parameter influencing the source (glacial melt), one that produces a diurnal pattern in the discharge record.

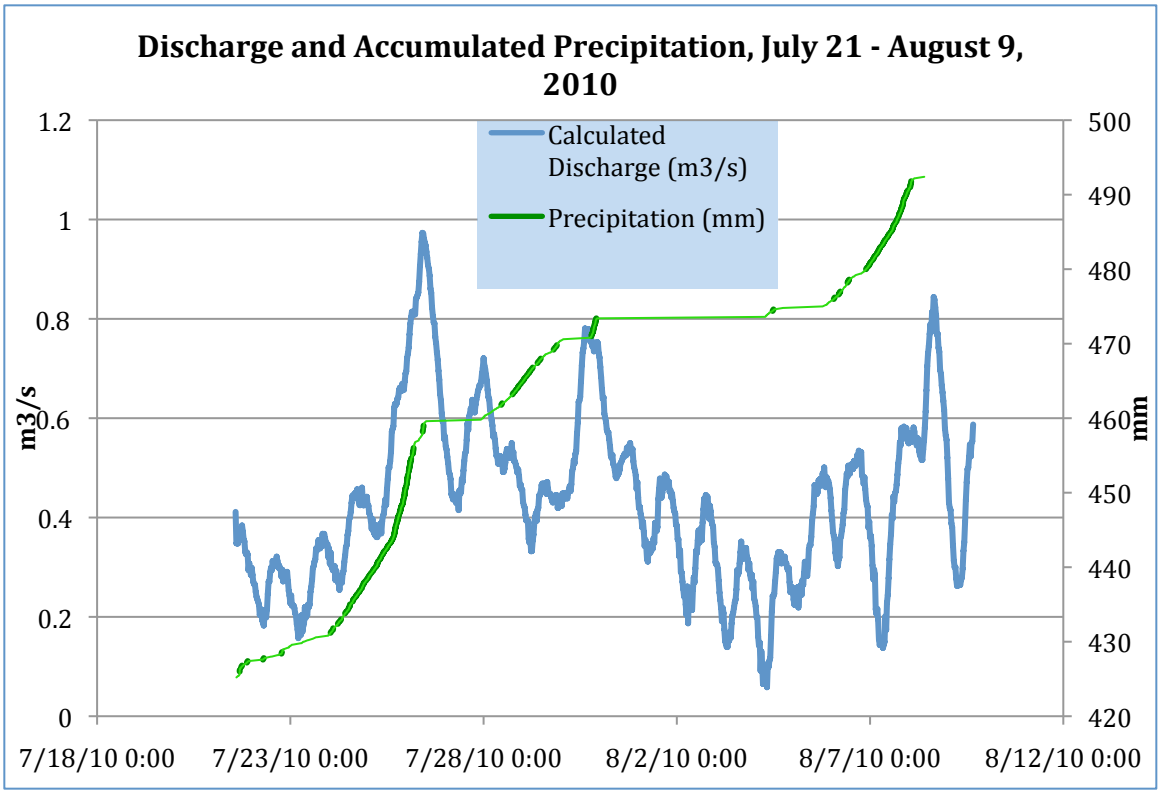

Figure 30: Graph showing the relationship between precipitation and discharge, note increasing discharge during precipitation events and decreasing and diurnal patterning during periods of no accumulation.

4.4. Discharge and Temperature

Having established precipitation as the main determinant of discharge, there must be a different climatic parameter influencing discharge during times of little or no precipitation. A graph of discharge and air temperature (Figure 31) shows the relationship between the two parameters. Though the temperature spike on July 25th at 08:00 precedes a matching spike in discharge, the increase in discharge comes more than 24 hours later on July 26th at 10:00 (Figure 31The other discharge highs and lows also exhibit similar lag times after temperature changes during the study period. Due to the proximity of the stage-recording site to the terminus of the glacier (~1.5 km), any changes that temperature might have on discharge should be recorded with a lag time of well under 24 hours. However, the diurnal patterning of the discharge record that does

not relate well to the highly variable temperature record suggests another factor influencing glacial melt.

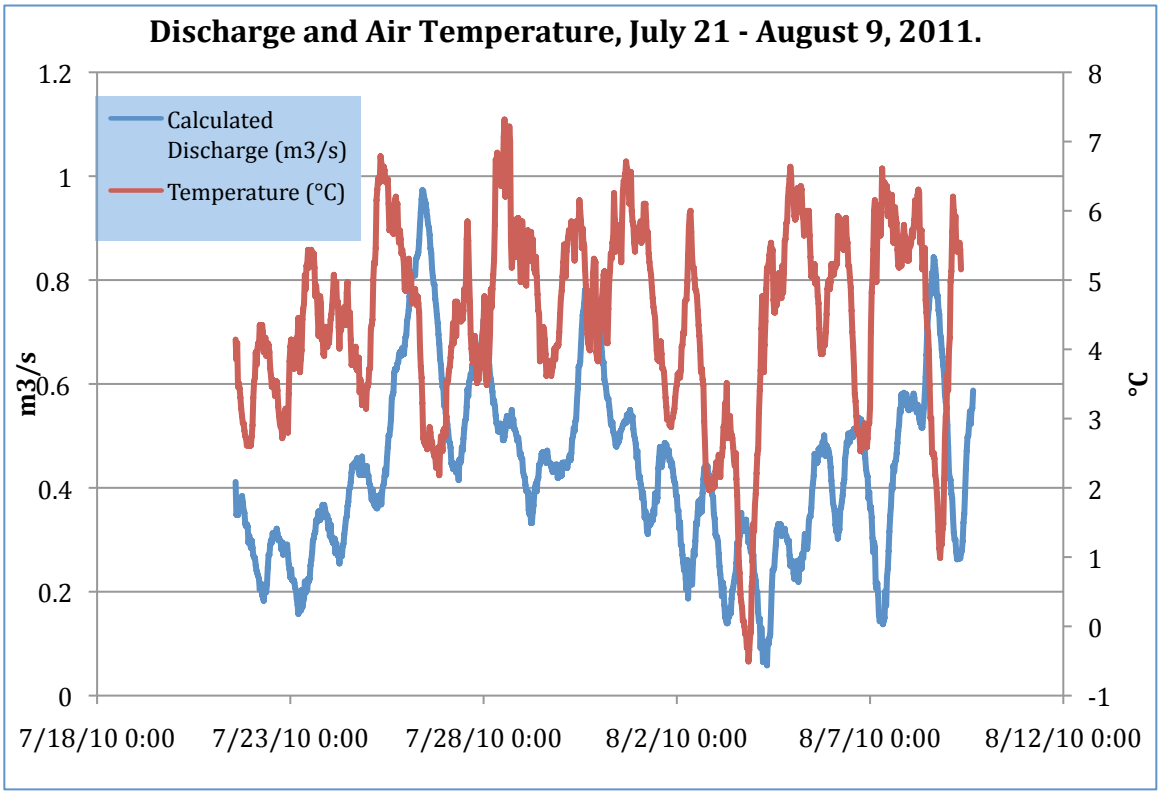

Figure 31: Graph of discharge and air temperature; notice lag time between temperature peaks as well as drop in temperature and drop in discharge late on August 3rd through early August 4th.

4.5. Discharge and Solar Radiation

Hess (1998) and Angstrom (1933) both noted the importance of radiation as an agent of glacier melt and contributor to discharge. During periods of little or no precipitation, solar radiation shows remarkable correlation to discharge, more so than air temperature. As seen in Figure 32, during the diurnal period of discharge from July 30th to August 4th, with little or no precipitation is, discharge shows high visual correlation to solar radiation

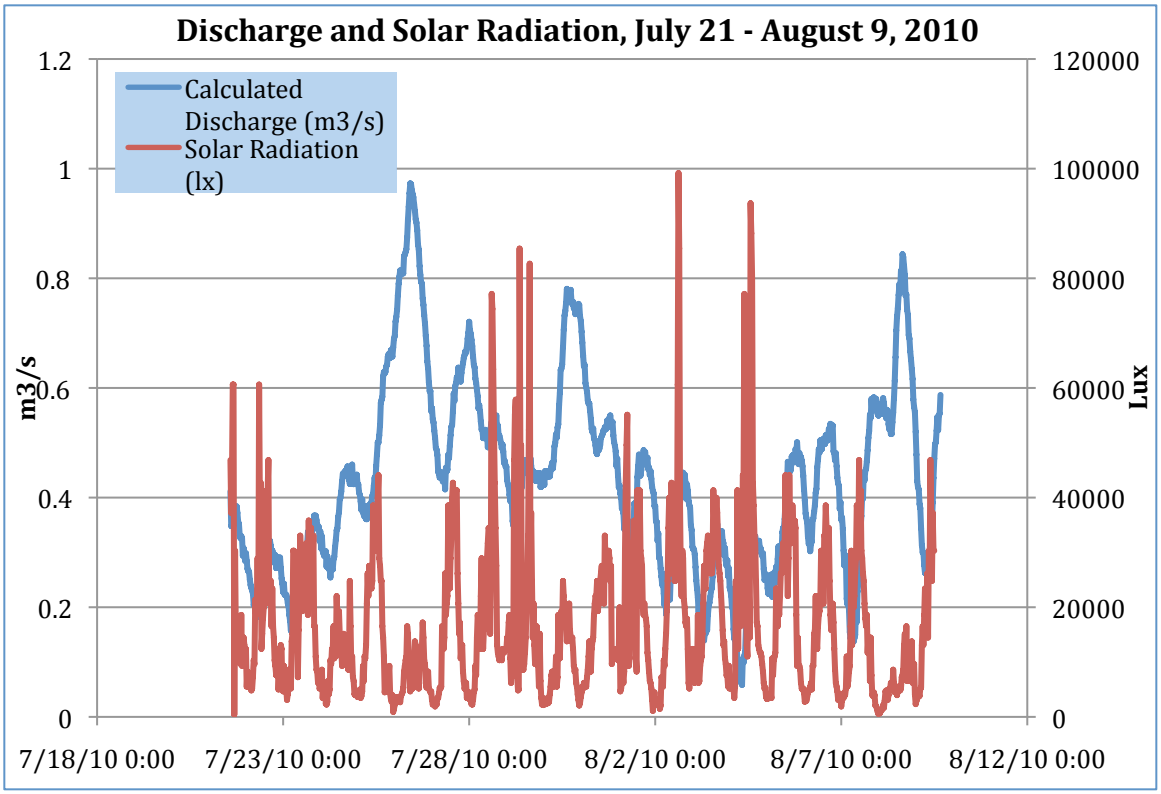

Figure 32: Graph showing discharge and solar radiation; low LX during high discharge due to cloud cover from precipitation events.

4.6. SSC and Precipitation

Having observed that discharge is the main controller of SSC, and that precipitation is the main determinant of discharge, it follows that precipitation will have the greatest influence on SSC. Figure 33 clearly shows the direct relationship between these two parameters, as precipitation accumulation events correlate well with the SSC events throughout the study period.

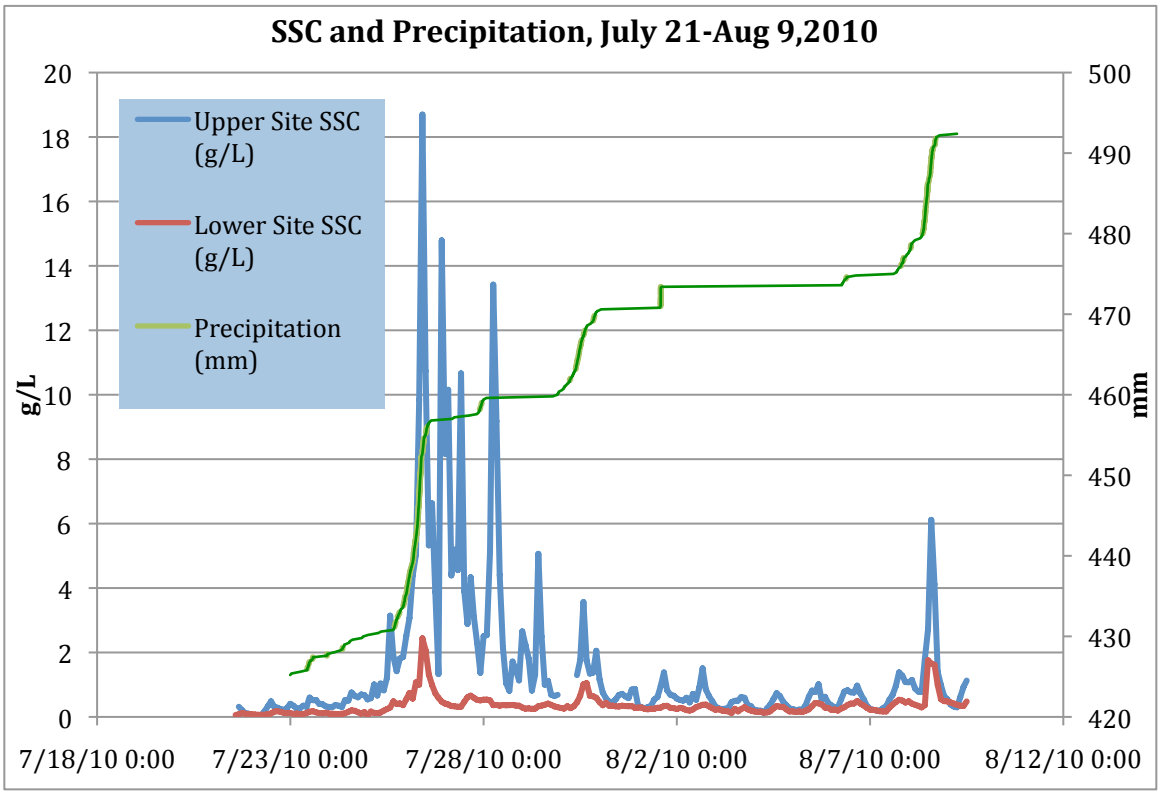

Figure 33: Graph relating SSC and accumulated precipitation for the field season.

The effect of precipitation on SSC and amount of sediment transported by the glaciofluvial system is twofold. Surface runoff adds directly to the discharge of the meltwater channel, increasing the stream's erosive power and increasing the suspended sediment load eroded from the stream channel. The grain size analysis of a high discharge event (Figure 26) shows an exponential increase in grain size during peaking discharge. This surface melt also carries with it sediment collected on the surface of the

glacier, though this amount is probably minimal in comparison to the secondary effect of precipitation (Hodgkins 1997). In polythermal glaciers like the Linné glacier, precipitation and surface melt that make their way down through the glacier and excavate subglacial sediment are responsible for the majority of the suspended sediment present in the meltwater channel (Hodgkins 1997; Jansson et al. 2005).

4.7. SSC versus Solar Radiation and Air Temperature

As observed from the discharge – solar radiation relationship, SSC shows little or no correlation to solar activity except during times of no precipitation when they both exhibit extremely close diurnal patterning (Figure 34).

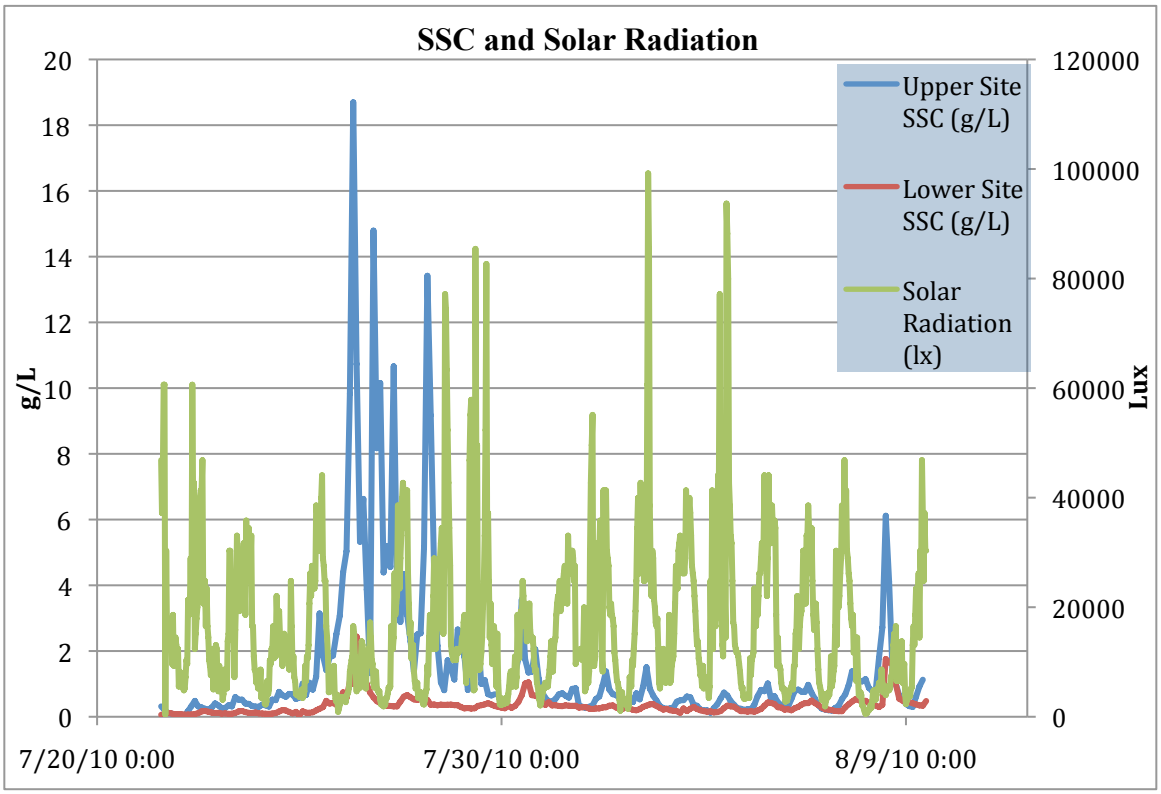

Figure 34: SSC and solar radiation during study period, note closely related diurnal patterning from August 1-7.

When comparing SSC and air temperature for the season, it becomes apparent that there is less of a relationship than between SSC and discharge. Figure 35 shows SSC and ambient air temperature. Though SSC shows some corresponding peaks to

temperature, the lag time (> 24 hours) significant. The below-freezing temperatures during the descending diurnal period on August 4th temporarily slowed melting rates and thus decreased meltwater input available to discharge.

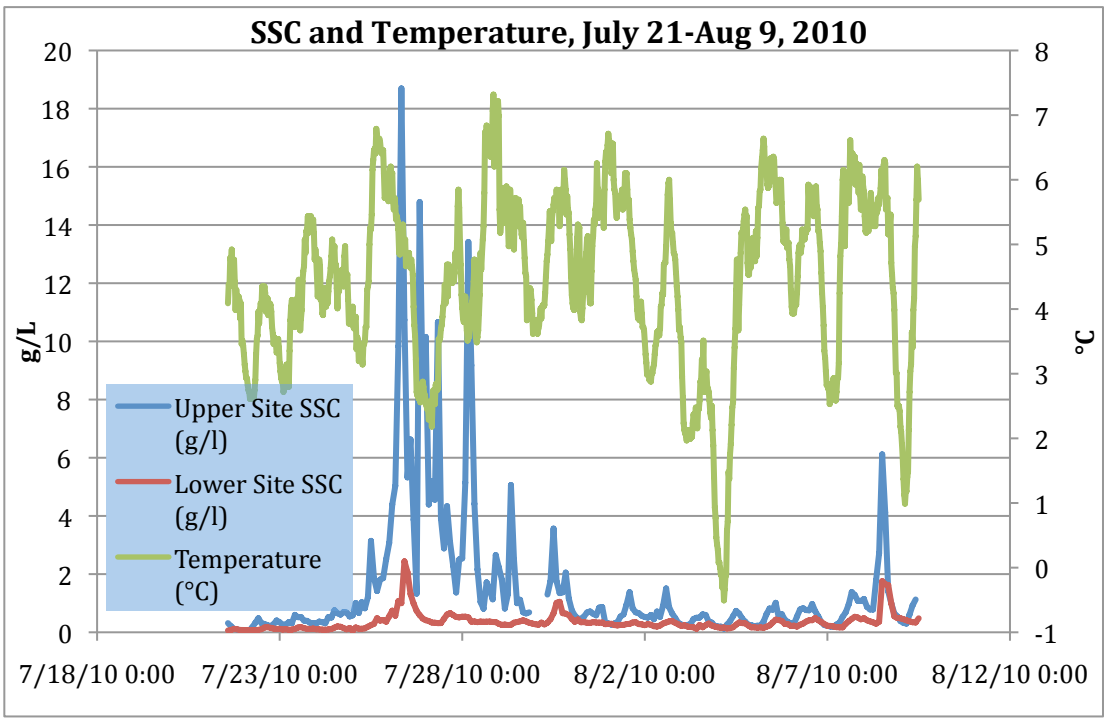

Figure 35: Graph of SSC and ambient air temperature for field season; note temperatures below freezing point and low point in SSC on August 4th.

4.8. Sediment Transport and Storage in a Glaciofluvial Environment

The second part of this project involved determining the parameters under which the glaciofluvial environment of Linné glacier operates. By understanding the processes that alter the sediment signal given off by the glacier, the record of climate in the sediment of lake Linné can be interpreted with more confidence. In terms of SSC, the Upper (proximal) sampling site shows a faster response time during increases in discharge, and close to an order of magnitude higher increase in SSC than the Lower (distal) site (Figure 15). Cumulative sediment yield also shows similar results, as the total of the Upper site (1437 metric tons) is more than four times the total of the Lower

site (318 metric tons) (Figure 16). With the amount of sediment input far exceeding the sediment output, the system acted as a sediment sink, retaining 1119 metric tons of sediment (an average of 58 metric tons per day) over the course of the study period. The sediment storage in the glaciofluvial system is in response to the loss of energy in the meltwater channel as its gradient lessens below the Upper site as well as deposition in two large braidplains present between the sampling sites (Figure 8, Figure 9). Work on the glacier Finsterwalderbreen by Hodgkins (2003) has shown that during particular weather conditions a glaciofluvial setting such as the Linné glacier can act either as a sediment sink or source. Further interference in the sediment signal from the glacier occurs when the spring melt the following year creates a high discharge flood event and excavates the sediment deposited in the sediment sink the previous year.

5. Conclusions

Throughout the study period from July 21st to August 9th, precipitation was the major influence on sediment production from Linné glacier and SSC in the glaciofluvial environment. Precipitation events caused the majority of glacier melt and as well as increased sediment production in the glacier system. During periods of little or no precipitation, solar radiation was determined to be the controlling factor on glacier melt and discharge, and therefore SSC and sediment production. The sediment signal produced by the glacier is more influenced by the precipitation than by other meteorological conditions (solar radiation, temperature). However, the lacustrine sediments at Lake Linné do not necessarily record what is occurring at the Linné glacier due to the nature of the transport environment immediately downstream of the glacier, which during the study period acted as a sediment sink. Well over half of the sediment load emanating from the glacier was deposited in large braidplains located between the Upper and Lower sites. A lowering of the gradient and the presence of two large areas of braided channel that reduce the velocity of the meltwater cause deposition in this glaciofluvial environment. This disruption of the sediment signal from the glacier changes the downstream lacustrine record by delaying sediment transport and deposition. It is proposed that trapped sediment does not make it down to Lake Linné until being excavated the following year by the high discharge spring melt, which flushes the entire system. This offset could potentially cause a year of lag between sediment production at the Linné glacier and sediment deposition in Lake Linné. The complications of the glaciofluvial environment coupled with the interferences of the Linné River as described

by Matell (2006) add another layer of disruption in the process of recording climatic conditions in lacustrine sediments downstream.

5.1. Future Work

In order to improve and build upon the results of this study, a longer field season covering the entirety of the melt season would be required. This study has provided a glimpse into the mechanisms and processes at work concerning climatic forcings on sediment production in a glaciofluvial environment. However, observing and recording the same conditions in the channel from the first flow to the last flow would produce a better understanding of sediment production and transport. Without observations of the spring melt event, a crucial link the transport of sediment to the Linné River goes unrecorded. By understanding sediment production throughout the entire cycle, a more coherent picture of glaciolacustrine relationships could be established.

Acknowledgments

I would like to thank the National Science Foundation (award #0649006) for making the Svalbard Research Experience for Undergraduates possible. Thanks go to Steve Roof and Al Werner for an exceptional program introducing geologic field research in the high Arctic to rising undergraduates. Thanks to University Centre in Svalbard (UNIS) for their logistical support and assistance in making this research possible. Thanks to Bob Carson for always asking the hard questions and pushing me to go further. Thanks to all of the 2010 Svalbard REU participants for assisting in the collection of data and carrying of water samples!

References Cited

Angstrom, A. (1933). "On the dependence of ablation on air temperature, radiation and wind." Geografiska Annaler 15: 264-271.

Apps, T. (2002). "Salinity - what do those figures mean?". Retrieved August 8, 2010, from http://www.appslabs.com.au/salinity.htm.

BBC (2010). "Svalbard." Retrieved 01/25, 2011, from http://newsimg.bbc.co.uk/media/images/42549000/gif/_42549857_norway1_arcticmap203.gif.

Boyum, A. and J. Kjensmo (1978). "Physiography and Linnévatn, Western Spitsbergen." Verh Internat Verein Limnol 20: 609-614.

Braun, C., D. R. Hardy, R. S. Bradley and M. J. Retelle (2000). "Streamflow and Suspended Sediment Transfer to Lake Sophia, Cornwallis Island, Nunavut, Canada." Arctic, Antarctic, and Alpine Research 32(4): 456-465.

Helfrich, E. P. (2007). Glacial Ablation Dynamics and Sediment Flux at Linnébreen, SPitsbergen. Department of Geosciences. Amherst, MA, University of Massachusetts.

Hess, H. (1998). "Die Gletscher." Braunschweig: Druck und Verlag von Friedrich Vieweg und Sohn: 426.

Hittson, T. (2010). Cryoconite Evolution and Formation on an Arctic Glacier Surface: A Case Study and Mode. Department of Geology. Chicago, IL., University of Chicago.

Hock, R. (2005). "Glacier melt: a review of processes and their modeling." Progress in Physical Geography 29: 362-391.

Hodgkins, R. (1997). "Glacier hydrology in Svalbard, Norwegian high Arctic." Quaternary Science Review 16: 957-973.

Hodgkins, R., R. Cooper, J. Wadham and M. Tranter (2003). "Suspended sediment fluxes in a high-Arctic glacierised catchment: implications for fluvial sediment storage." Sedimentary Geology 162: 105-117.

Hodson, A. (1994). Climate, hydrology, and sediment transfer process interaction in a sub-polar glacier basin, Svalbard. Department of Geology. Southhampton, University of Southhampton.

Ingólfsson, Ó. (2004). "Outline of the geography and geology of Svalbard." University Center in Svalbard 2005.

Jansson, P., G. Rosqvist and T. Schneider (2005). "Glacier fluctuations, suspended sediment flux and glaciolacustrine sediments." Geografiska Annaler 87: 37-50.

Mangerud, J. and J. I. Svendsen (1990). "Deglaciation chronology inferred from marine sediments in a proglacial lake basin, western Spitsbergen, Svalbard." Boreas 19: 249-272.

Matell, N. (2006). Undergraduate Thesis. School of Natural Sciences. Amherst, MA, Hampshire College.

Overpeck, J., K. Hughen, D. Hardy, R. Bradley, R. Case, M. Douglas, B. Finney, K. Gajewski, G. Jacoby, A. Jennings, S. Lamoureux, A. Lasca, G. MacDonald, J. Moore, M. Retelle, S. Smith, A. Wolfe and G. Zielinski (1997). "Arctic enviromental change of the last four centuries." Science 278: 1251-1256.

Perreault, L. M. (2006). "Mineralogical Analysis of Primary and Secondary Source Sediments to Linnévatnet, Spitsbergen, Svalbard." Department of Geology B.Sc. Thesis: Bates College, Lewiston, Maine.

Rantz, S. E. and others (1983). USGS Streamflow Manual - Stage and Discharge Measurement. USGS. Washington, United States Government Printing Office.

Schiff, K. (2004). "Unsustainable Glacier Ablation at 78°N Latitude, Linnébreen, Svalbard." Department of Geological Sciences B.Sc. Thesis: Indiana University, Bloomington, Indiana.

Snyder, J. A., A. Werner and G. H. Miller (1999). "Holocene cirque glacier activity in western Spitsbergen, Svalbard: sediment records from proglacial Linnévatnet." The Holocene 10: 555-556.

Stewart, H. A. (2007). Evidence for Accelerated Surface Melting Rates on the Linné Glacier, Svalbard. Department of Geology. Dayton, University of Dayton. Undergraduate.

Thasler (2010). "Svalbard." Retrieved 01/25, 2011, from http://people.ucsc.edu/~%20thasler/svalbard-map.

Werner, A. (1993). "Holocence Moraine Chronology, Spitsbergen, Svalbard: Lichonometric Evidence for Multiple Neoglacial Advances in the Arctic." The Holocene 3: 128-137.